W-PM-A1 RAMAN SPECTROSCOPY: A NEW METHOD OF PROBING THE CONFORMATION OF MYOSIN. E. Bayne Carew*, Irvin M. Asher, and H. Eugene Stanley, Harvard-M.I.T. Program in Health Sciences and Technology, M.I.T., Cambridge, Mass. 02139.

The myosin molecule, which consists of two globular head regions attached to a coiled-coil α-Helical rod, has been studied by Raman spectroscopy with particular emphasis on the conformationally-sensitive amide III region of the spectrum. The peaks near 1244 cm^{-1} have been assigned to β-pleated and random coil structures; peaks at 1265 and 1304 cm^{-1} have contributions from both α-helical structure and C-H bending vibrations. These bands (which cannot be accounted for on the basis of amino acid spectra alone) include amide III vibrational modes, since low frequency activity appears on deuteration of the NH groups. Subtraction of spectra in D_2O from spectra in H_2O--with due consideration of Raman scattering efficiencies--permits an estimate of the relative α,β, and random coil structures. Changes in protein structure are reflected in changes in the Raman spectra. Increasing the temperature from 20 C to 68 C increases the intensity of the 1244 cm^{-1} band, as might be expected on denaturation. The addition of 100 μM $MgCl_2$ dramatically increases the intensity at 1304 cm^{-1} with respect to the 1004 cm^{-1} Phe and the 1455 cm^{-1} CH bending vibrations; the involvement of the amide III regions in this $MgCl_2$-induced effect is shown by the shift of this intensity to lower frequency upon deuteration. The $MgCl_2$ effect occurs on a slow time scale.

Supported by the Research Corporation and the NIH(HL-143220). E.B.C. was supported by the U. of Michigan while on sabbatical leave.

W-PM-A2 RAMAN SPECTROSCOPIC STUDY OF THE TRYPTIC SUBFRAGMENTS OF MYOSIN. E.B. Carew*, J.C. Seidel, I.M. Asher, H.E. Stanley, A. Hewitt*, J.D. Potter and J. Gergely, Harvard-MIT Program in Health Sciences and Technology; Dept. Nat. Sci., Univ. Michigan, Dearborn; Dept. Muscle Res., Boston Biomed. Res. Inst.; Dept. Neurol., Mass. Gen. Hosp.; and Dept. Neurology and Biological Chemistry, Harvard Med. School, Boston Massachusetts.

Light meromyosin (LMM), heavy meromyosin (HMM), HMM subfragment-1 (S-1), and HMM subfragment-2 (S-2) show characteristic Raman spectra. This is most apparent in the conformationally-sensitive amide III region (from 1220 to 1320 cm^{-1}). LMM, which is almost completely α-helical and a dimeric coiled coil,has a strong peak at 1304^{-1} cm^{-1}. S-1 has a peak near 1265 cm^{-1} attributable to its α-helical component (~40%); it also has a broad 1244 cm^{-1} band, generally assigned to random coil and β-pleated structures. HMM is heterogeneous in structure, with its globular S-1 portions attached to the rod-like α-helical S-2. The HMM spectrum shows a strong 1304 cm^{-1} peak, as well as a weaker peak at 1265 cm^{-1}, both characteristic of α-helical structures; bands near 1244 cm^{-1} (random coil and/or β structure) are also apparent in HMM. In the light of these results the 1304 and 1265 cm α-helical peaks can be assigned to the rod-like and globular portions, respectively, of the myosin molecule. Denaturation increases the strength of the 1244 cm^{-1} peak in all preparations at the expense of the 1265 cm^{-1} and 1304 cm^{-1} bands. (Supported by grants from the Research Corporation, NIH (HL-14322, HL-5949, HL-15391, SO1 RR 05711), the National Science Foundation, American Heart Association and Muscular Dystrophy Associations of America, Inc. J.P. is an Established Investigator of the American Heart Association)

W-PM-A3 INTRAMOLECULAR DISULPHIDE FORMS OF LC_2 LIGHT CHAIN OF RABBIT SKELETAL MYOSIN IN NATIVE HEAD AND PURIFIED SUBUNIT. S. Sarkar, S. P. Mukherjee* and A. Sutton*, Dept. Muscle Res., Boston Biomed. Res. Inst. and Dept. Neurology, Harvard Med. School, Boston, Mass. 02114.

When samples of rabbit skeletal myosin (M), preserved at 0° for a week or more in buffers containing 0.5 M KCl, are analyzed by SDS-gel electrophoresis, an additional band associated with LC_2 light chain and having a faster mobility is obtained. Reduction of M with 25-50 mM DTT before SDS treatment or carboxymethylation of M with iodoacetamide prevents the formation of the faster band. When air is blown to the surface of fresh samples of M at 0° for 10 min before SDS treatment, the LC_2 band is almost completely converted into the faster band. Treatment of this air-oxidized M with DTT prior to electrophoresis reverses the band pattern. Densitometric scannings of gel runs of M show that the faster band was derived from LC_2, presumably forming species with intramolecular S-S crosslinks (Griffith, I.P., Biochem. J. 123, 556, 1972). M purified by chromatography on DEAE-cellulose also exhibits this reversible oxidation-reduction of LC_2, indicating that the band with faster mobility is not due to impurities. LC_2 containing S-S crosslinks is more resistant to removal from M by treatment with 5-5'-dithiobis(2-nitrobenzoic acid) than LC_2 in the reduced state. This double band pattern in SDS-gel runs is also shown by isolated samples of highly purified LC_2. The crosslinking of LC_2 has no effect on myosin ATPase activity. These results indicate that the two -SH groups in LC_2 can form intramolecular crosslinks both in the native myosin head and isolated subunit. (Supported by grants from NIH, AM-13238; American Heart Association, 71-915, and the Muscular Dystrophy Associations of America, Inc.)

W-PM-A4 THE ROLE OF BOUND NUCLEOTIDES IN THE POLYMERIZATION OF ACTIN. Roger Cooke, Dept. of Biochemistry, University of Ca., San Francisco 94143

Each actin monomer binds one nucleotide (ATP or ADP). Bound ATP is dephosphorylated when the actin is polymerized. An unsplitable analog of ATP, AMPPNP, can also bind to actin monomers, and radioactive analog was shown to be incorporated into the actin polymer. The polymerization, assayed by the change in OD_{232}, followed a simple expotential in all cases studied. The rate of polymerization was similar for bound ATP and AMPPNP; both of which were 3 to 5 times faster than for ADP. The concentration of actin monomers in equilibrium with the polymer when the polymerization has reached steady state, $[G_\infty]$, was determined by measuring the amount of polymer formed as a function of the actin concentration. Values of G_∞ were found for different bound nucleotides to be: $G{\cdot}ATP_\infty$ = .7μM, $G{\cdot}AMPPNP_\infty$ = .8 μM and $G{\cdot}ADP_\infty$ = 3.4 μM. It can be shown that the equilibrium constant of the polymerization is given by $K=[G_\infty]^{-1}$ for the case in which no nucleotide is split. The polymerization of actin ATP is more complex, but the values of the rate and G_∞ could be explained by a simple kinetic scheme in which the nucleotide dephosphorylation occurs in a step following the polymerization step. The conclusions to be drawn from these studies are: (1) the binding of ATP to the actin monomer promotes the polymerization slightly more than does the binding of ADP, (2) less than 1 Kcal/mole of the free energy of the bound ATP is used to promote the polymerization, (3) the splitting of the nucleotide plays no role in the polymerization. Thus it appears that the bound nucleotide may be used in some interaction other than polymerization. Such a role is suggested by our recent observation that AMPPNP bound to F actin inhibits the velocity of superprecipitation with myosin.

This study was supported by grants from NSF (GB 2499x) and USPHS (AM17559).

W-PM-A5 A STUDY OF THE POLYMERIZATION OF G-ADP-ACTIN. James E. Estes, Department of Biology, Rensselaer Polytechnic Institute, Troy, New York.

In an earlier hydrostatic pressure study (Fed. Proc. 33, 1522, 1974), it was found that the polymerization of G-ATP-actin is accompanied by a volume change of activation (ΔV^*) of about 100 cc/mole. To determine whether this ΔV^* is due to conformational changes in the monomer subunits or to the hydrolysis of the actin-bound ATP, the effect of hydrostatic pressure on the polymerization of G-ADP-actin was examined. While the G-ATP-actin from which G-ADP-actin was prepared had a specific viscosity (η_{sp}) around 0.008, G-ADP-actin routinely had a η_{sp} about twice as great, suggesting the presence of nuclei. The addition of low concentrations of salt to G-ADP-actin at 25°C affected a moderate rate of polymerization which was followed by viscometry. When the η_{sp} attained a value around 0.1 (indicating the presence of short polymers), a portion of the sample was placed under hydrostatic pressure. Following 10 minutes of pressure treatment, the rate of polymerization of the pressure sample was determined and compared to that of the atmospheric control. Both samples were then brought to 0.1M KCl and allowed to polymerize fully. In the pressure range 100-600 kg/cm^2, the application of pressure had no effect on the rate of polymerization, and thus under these conditions, there apparently is no ΔV^* associated with the addition of ADP-actin monomers to the nuclei or short polymers present. At pressures near 700 kg/cm^2, polymerization was completely stopped, and at higher pressures (800-1000 kg/cm^2) depolymerization appears to occur. The final η_{sp} of all samples was similar indicating the pressure effect was reversible. Since the difference in the ΔV^* for the polymerization of the two types of actin is much greater than the ΔV^* for ATP hydrolysis alone, the ΔV^* previously obtained for the polymerization of monomeric G-ATP-actin is apparently due to conformational changes in the actin monomer and/or bound water changes. Supported by the Heart Assn. of Eastern New York.

W-PM-A6 DETERMINATION OF THE DISSOCIATION CONSTANT OF THE ACTO-S1 "RIGOR" COMPLEX.

S. Marston & A. Weber, Department of Biochemistry, University of Pennsylvania Medical School, Philadelphia, Pa. 19174.

We measured the binding constant of 1-^{14}C Iodoacetamide labelled HMM-subfragment-1 (^{14}C-S1) to F-actin by sedimenting acto-S1 for 2 hours at 50,000 x g and assaying the radioactivity remaining in the supernatant. The apparent binding constants were 1,1 and 0.4 x 10^7 M^{-1} for pure actin and 0.5, 0.4, 0.06 x 10^7 M^{-1} for regulated actin at .027, .08, and .14 ionic strength respectively (pH 7.0, 25°C). Measurements of the displacement of ^{14}C-S1 from actin by native S1 showed that labelling had not altered the apparent dissociation constant. Our binding constants are minimal values because we assumed that all of the supernatant S1 and all of the actin in excess of sedimented S1 was free and active. However, control experiments showed that at these low actin concentrations not all of the actin sediments and furthermore the data suggested that some of the supernatant S1 was bound to supernatant actin and not free. Therefore, the values we used for our calculations of free S1 were too high giving too low a binding constant. The calculated constant would be too low also if some of the supernatant actin were inactive. The artifact of supernatant actin is minimized at high ratios of S1 / actin (0-100 nM actin, 30 nM S1) where no less than 75% of the actin sediments and our constants were calculated in this range of protein concentrations.

W-PM-A7 FLUORESCENCE STUDIES OF THE INTERACTION OF 1,N^6-ETHENOADENOSINE PHOSPHATES WITH ACTIN. Stephen C. Harvey, Herbert C. Cheung and Kenneth E. Thames. Department of Biomathematics, University of Alabama in Birmingham, Birmingham, Alabama 35294.

1,N^6-ethenoadenosine triphosphate (ϵ-ATP) binds to G-actin, and the ϵ-G complex possesses full polymerizability, giving ϵ-ADP bound to F actin. We have investigated the fluorescence properties (absorption, emission, and excitation spectra; lifetimes; quantum yields; fluorescence depolarization) of ϵ-ATP bound to G actin and of ϵ-ADP bound to F actin. The interaction of ϵ-ADP-F actin with myosin has also been studied. The observed lifetimes are: τ(ϵ-ADP) ~ τ(ϵ-ATP) = 25 nsec; τ(ϵ-ATP-G actin) = 36 nsec; τ(ϵ-ADP-F actin) = 33 nsec; τ(ϵ-ADP-actomyosin) = 31 nsec. The large increase in lifetime on binding of the ϵ nucleotides is, as far as we know, peculiar to the interaction of the nucleotides with actin, for it is not observed in the interactions of ϵ nucleotides with other proteins. The effect is not due to polarity of the environment, microviscosity, hydrogen bonding, change in quenching by O_2 or H_2O, or to a simple interaction between the base and an amino acid side chain. A possible explanation is that the nucleotide, which exists in the anti conformation in solution, is forced into the syn conformation on binding to actin.

W-PM-A8 CA^{2+}-INDUCED COIL TO HELIX TRANSITION OF TROPONIN C IN UREA. B. Nagy, J.D. Potter, and J. Gergely, Dept. of Muscle Res., Boston Biomedical Research Institute; Dept. of Neurology, Massachusetts Gen. Hospital; and Depts. of Neurology and Biol. Chem., Harvard Med. Sch., Boston, Mass.

Titration with Ca^{2+} of two high affinity binding sites of TnC out of a total of four (see Potter and Gergely, Fed. Proc. 33, 146, 1974) produces an increase in CD from $[\theta]_{222}$= -9,200 to -14,800, indicating an increase in α-helix content. In 6M urea and 1 mM EDTA $[\theta]_{222}$ = 0, but titration with Ca^{2+} produces $[\theta]_{222}$ = -5,200. Thus the change in $\Delta[\theta]_{222}$ produced by Ca^{2+} is about the same with native TnC and in 6M urea. Calcium produces the same changes in the UV absorption spectrum indicative of a less polar environment of phenylalanine residues, leading to an optically active absorption band, with native TnC and in 6M urea. Urea does not affect the reversibility of the CD and absorption changes produced by Ca^{2+} upon its chelation by EDTA. The reduced reactivity of the single -SH group of TnC towards thiol reagents (cf. Potter et al., Fed. Proc. 32,569, 1973; and Potter, these Abstr.) in the presence of Ca^{2+} or Mg^{2+} is also present in urea. The fact that certain effects of Ca^{2+} on optical and chemical properties of TnC described above are present in 6M urea suggests that Ca^{2+} exerts an effect on a region of the molecule adjacent to a binding site. The α-helical segment adjacent to one of the Ca^{2+} binding sites containing two phenylalanine residues and the single cysteine residue (cf. Collins et al., FEBS Lett. 36, 268, 1973) are likely to be part of the α-helical domain stabilized by Ca^{2+} in urea. (Supported by grants from NIH (HL-5949, SO1 RR 05711), NSF (GB43484, GB38380) and MDAA. J. P. is an Established Investigator of the American Heart Association)

W-PM-A9 THE EFFECT OF CA^{2+} AND MG^{2+} ON THE REACTIVITY OF THE CYSTEINE RESIDUE IN TROPONIN C. James D. Potter, Dept. of Muscle Res.,Boston Biomedical Research Inst.; and Dept. of Neurol., Harvard Med. Sch., Boston,Ma.

Reaction of the single cys of troponin C (TnC) with an iodoacetamide spin label is greatly inhibited in the presence of Ca^{2+} or Mg^{2+} (Potter et al., Fed. Proc. 32, 569,1973). TnC contains two high affinity (10^7 M^{-1}) Ca^{2+} binding sites that bind Mg^{2+} competitively, and two Ca^{2+} binding sites of lower affinity (10^5 M^{-1}) that do not bind Mg^{2+} (Potter and Gergely, Fed. Proc. 33,146,1974). To determine whether one or more of these Ca^{2+} binding sites is involved in the change in reactivity of the -SH group the rate of the reaction of DTNB with the -SH group was studied as a function of pCa in the presence and absence of Mg^{2+}. In its absence there was a large decrease in the rate of the reaction on increasing $[Ca^{2+}]$ from 10^{-9}-10^{-7}M. The data are consistent with binding of Ca^{2+} to either high affinity site producing the change. With 2 mM Mg^{2+} when the high affinity Ca^{2+} sites are nearly saturated with Mg^{2+}, the reaction rate was almost as low as with high Ca^{2+} in the absence of Mg^{2+} and did not change with pCa. Large increases (20%) in the α-helical content of TnC occur upon binding of either Ca^{2+} or Mg^{2+} to the high affinity sites. Sequence comparisons (Collins et al., FEBS Lett. 36, 268,1973) of TnC and carp muscle calcium binding protein, whose three-dimensional structure is known, suggest that the single -SH group in TnC is located in an α-helical region adjacent to one of the Ca^{2+} binding sites. The change in accessibility of the -SH to DTNB could be due to the formation of the α-helix in the region containing the -SH group or to a change in tertiary structure involving another segment of the sequence. (Supported by NIH, NSF and Mass. Hrt. Assoc.; and Established Investigatorship,Amer. Hrt. Ass)

W-PM-A10 THE EFFECT OF CALCIUM AND OTHER DIVALENT CATIONS ON THE CONFORMATION OF BOVINE CARDIAC TROPONIN. Tsung-I Lin and Joseph Y. Cassim, Department of Biophysics, Ohio State University, Columbus, Ohio 43210

Bovine cardiac troponin was prepared by the method of Tsukui and Ebashi (J.Biochem.,73 1119(1973))with minor modifications. The crude troponin was purified by repeated acidic precipitation at pH 2.3-4.2 and ionic strength of 0.8-1.2, which effectively removed most of the major contaminants. Further purification of troponin was achieved by column chromatography on DEAE-Cellulose and DEAE-Sephadex. Polyacrylamide gel electrophoresis of purified troponin in the presence of SDS showed three bands with molecular weights of approximately 38,000,26,000 and 18,000. The biological activity of troponin was assayed by Ca^{++}-sensitivity of superprecipitation and ATPase of actomyosin. The effect of Ca^{++} on the conformation of troponin was studied by circular dichroism (CD) of troponin in the presence of various concentrations of Ca^{++} adjusted by EGTA-Ca^{++} buffers. In the far-UV region, 200-250 nm,CD of troponin exhibited two extrema of about equal ellipticity (1.5×10^4 deg·cm^2/dmole) at 222 and 209 nm, indicative of the presence of some ordered secondary structures. Addition of Ca^{++} caused a 3-4% increase of ellipticity at 222 nm but no change at 209 nm. Similar result was obtained with the addition of some other divalent cations. In the near-UV region,250-325 nm, CD of troponin exhibited several extrema which can be correlated with the maximum and shoulders found in absorption spectrum in the same region. Addition of Ca^{++} caused no significant change in ellipticity or position of these extrema. These observations are not in accord with any model of the calcium control mechanism of myocardiac contractility which requires calcium induced global conformational changes of cardiac troponin. This study has been supported by a grant (#73-41) from The Central Ohio Heart Association.

W-PM-A11 RAMAN SPECTRA OF TROPOMYOSIN, AND TROPONIN AND ITS SUBUNITS - THE EFFECTS OF CA^{++} AND MG^{++}. E.B. Carew*, J.D. Potter, I.M. Asher, H.E. Stanley, J.C. Seidel and J. Gergely (Intr. by S.S. Lehrer), Harvard-MIT Program in Health Sciences and Technology; Dept. Nat. Sci., Univ. Michigan, Dearborn; Dept. Muscle Res., Boston Biomed. Res. Inst.; Dept. Neurol., Mass. Gen. Hosp.; and Dept. Neurol. and Biol. Chem., Harvard Medical School, Boston Mass.

Raman spectra of tropomyosin (TM), troponin (Tn), and the three subunits of Tn (TnC, TnI and TnT) are reported, with particular emphasis on the conformationally sensitive amide III region. The spectrum of TM, a coiled-coil α-helical protein, has strong peaks at 1304 and 1308 cm^{-1};these shift upon deuteration to lower frequencies, thus demonstrating the presence of amide III α-helical contributions to these peaks. TnT, the TM binding subunit of Tn, has a strong peak at 1304 cm^{-1}, indicative of α-helical structure. Three peaks appear between 1220-1250 cm^{-1}, whose contributions from β-pleated and random coil structures are expected. TnC, the Ca^{++} binding subunit, has a weaker peak near 1304 cm^{-1}, with a strong peak at 1262 cm^{-1}, both of which may reflect α-helical structure. Unlike Mg^{++}, Ca^{++} induces a strong peak at 1232 cm^{-1}, as well as some intensification in the 1262 and 1304 cm^{-1} regions. TnI, the inhibitory subunit, has very strong peaks between 1220 and 1250 cm^{-1}, with very little α-helical contribution near 1304 cm^{-1}. The relationship of spectra of Tn to those of its components, both in the presence and absence of Ca^{++} and Mg^{++}, is currently under investigation. (Supported by grants from the Research Corporation, NIH (HL-14322, HL-5949, HL-15391, SO1 RR 05711), the National Science Foundation, American Heart Association and Muscular Dystrophy Associations of America, Inc. J.P. is an Established Investigator of the AHA)

W-PM-A12 CHARACTERIZATION OF THE TROPONIN-TROPOMYOSIN COMPLEX FROM EMBRYONIC CHICKEN MUSCLES. Raman K. Roy, James D. Potter and S. Sarkar. Dept. Muscle Res., Boston Biomed. Res. Inst. and Dept. Neurology, Harvard Med. School, Boston, Mass. 02114.

Due to the high nucleic acid content of embryonic muscles, the conventional method for the isolation of the regulatory complex, troponin-tropomyosin (Tn-TM), using $(NH_4)_2SO_4$ fractionation was found to be very unsatisfactory in our hands. We have developed a method for the isolation of the regulatory complex, free of other contractile proteins, from embryonic chicken muscles by chromatography on a column of DEAE-cellulose. When a crude KCl extract (Greaser and Gergely, J. Biol. Chem. 246, 4226, 1971) of dried ether powder of muscle was run on a DEAE-cellulose column equilibrated with 0.1 M KCl and 50 mM Tris, pH 8.0, most of the protein appeared in the void volume. On subsequent elution of the column with a linear gradient of KCl (0.1-0.5 M), the whole complex, Tn-TM, was eluted at about 0.22 M KCl concentration. Quantitation using scanning of SDS-gel runs of the complex showed that the polypeptide components (TnT, 44,000 daltons; TnI, 24,000 daltons; TnC, 19,000 daltons; TM, 33,500 daltons) were present in the same molar ratio as in the adult regulatory complex (1:1:1:2). The isolated Tn-TM from 14-day embryonic leg and breast muscles was as effective as that obtained from rabbit muscles in conferring Ca^{2+} sensitivity when tested on the ATPase activity of reconstituted adult rabbit actomyosin. These results indicate that in a 14-day old embryonic muscle all the regulatory proteins are assembled as a functional Tn-TM complex. (Supported by grants from NIH, AM-13238; the Massachusetts Heart Association # 1181, and the Muscular Dystrophy Association of America, Inc. J.D.P. is an Established Investigator of the American Heart Association.)

W-PM-A13 INHIBITION OF CALCIUM-BINDING OF TROPONIN BY GENERAL ANESTHETICS. Tsuyoshi Ohnishi, Andrew D. Brotman* and Henry L. Price*, Biophysics Laboratory, Department of Anesthesiology, Hahnemann Medical College, Philadelphia, Pa. 19102

The mechanism of anesthetic-induced myocardial depression is still unsolved. From ATPase studies, we have suggested that general anesthetics can interact directly with regulatory proteins(tropomyosin-troponin) of heart muscle and cause myocardial depression(Biochemistry/Biophysics 1974 Meeting; Biochem. and Biophys. Res. Comm., 57, 316, 1974). Using myofibrils prepared from dog ventricles and ^{45}Ca, we have found that both halothane and diethyl ether can supress the Ca-binding of myofibrils considerably at the clinically useful concentration. By purifying troponin from the same preparation, we have found that Ca-binding of troponin is supressed about 60 % at pCa = 4.5 by halothane(2 % v/v gas). Since the binding of Ca^{++} to troponin represents an essential link in muscle contraction, these results suggest the ability of anesthetics to depress this binding may account for their effect on contractile force.

W-PM-B1 MEMBRANE IMPEDANCE OF SQUID AXON DURING HYPER- AND DEPOLARIZATION. S. Takashima and H. P. Schwan, Department of Bioengineering, University of Pennsylvania, Phila., Pa. and K. S. Cole, Laboratory of Biophysics, National Institute of Health, Bethesda, Md.

Membrane capacitance and conductance of squid axons were measured in the presence of depolarizing and hyperpolarizing command pulses. Two Pt-Ir internal electrodes were used, the one for the application of pulses and the other for the measurements of membrane capacitance and conductance. A glass canulla filled with KCl-agar was also inserted in order to monitor the membrane potential. The duration and levels of depolarizing and hyperpolarizing potentials were 20-40 msec and 0 to 60 mv. The frequency range for the admittance measurement was from 1KHz to 50KHz. The bridge was prebalanced for the resting membrane and the disturbance of the bridge upon application of command pulses was displayed on an oscilloscope. The admittance was measured after all the transient phenomena including action potential were subsided and the membrane potential reached a steady state value. We observed that the membrane resistance increased upon hyperpolarization and approached asymptotically to a limiting value. On the other hand, the membrane resistance decreased, as expected, upon depolarization. In neither case, the membrane capacitance changed more than 5-10 percent. This research is partially supported by NSF GK-40119 and NIH HE-01253.

W-PM-B2 RESISTIVITY OF EXTRUDED SQUID AXOPLASM. K. S. Cole, Laboratory of Biophysics, IR, NINDS, National Institutes of Health, Bethesda, Md. 20014 and the Marine Biological Laboratory, Woods Hole, Mass. 02543.

Values of electrical resistivity of squid axoplasm from one to 6.9 times sea water obtained by six different methods, suggested another attempt. A 100 μm platinized electrode was to be inserted from each end of an axon in iso-osmotic sucrose and impedance between them measured as a function of their separation. But observations that the resistance of axons in sucrose increased steadily ruled this out. Axoplasm from 2 or 3 axons was transferred to a glass capillary, 0.6 mm i.d., and the 1 kHz series resistance and reactance were measured at electrode separations from 16 mm to 2 mm. The resistance was linear vs. distance-to give the resistivity-and the reactance nearly constant-to imply that the electrode contributions did not vary. Frequency runs from 10 Hz to 30 k Hz at 10 mm gave electrode impedance of the form $(j\omega)^{-\alpha}$ and showed a possible 1-2% effect on the axoplasm resistivity results. In nine experiments, after one was discarded for cause, the range and average resistivities were, respectively, 1.2 to 1.6 and 1.4 times those of artificial sea water, with 19.7 Ω cm at 24.4°C median values. No single cause for the variability was apparent. These experiments essentially confirm the means and variations of two early experiments with intact axons and recent results with a single internal electrode to give an over-all average resistivity of 1.4 ± 0.2 times sea water. But this figure gives no obvious indication of the axoplasm resistivity in an intact animal.

W-PM-B3 ESR SPIN LABEL MEASURE OF VISCOSITY OF MAMMALIAN NERVE AXOPLASM. R. Haak, Med. Biophy., Ind. U. Sch. Med., F. Kleinhans*, Phys. Dept., IUPUI and S. Ochs, Dept. Physiol., Med. Biophy., Ind. Sch. Med., Indpls., Ind.

An understanding of axoplasmic transport in nerve is dependent on a knowledge of axoplasmic viscosity. However, measurements of viscosity have only been carried out to a limited extent in giant nerve fibers. To measure the viscosity of the smaller fibers of cat sciatic nerve, we have utilized tempone labeling and ESR. The excised nerves were kept at 38°C in isotonic sucrose bubbled with a 95/5 O_2/CO_2 gas mixture for 1 hr, and transferred to an oxygenated isotonic 0.11 M $NiCl_2$ solution (310 mOsM) containing 5 mM tempone. After allowing 5-15 min for labeling, the nerve was inserted into a 4 mm ID quartz tube containing a small amount of the same solution. The tube was oxygenated, capped and an ESR spectra obtained. Nerves subjected to these procedures retain the function of fast axoplasmic transport. A characteristic nitroxide spin label spectra was observed which decayed due to a reduction of the spin label by reducing agents present inside the cell. The signal due to the spin label on the outside surface or in the extracellular space was greatly reduced by the line broadening effects of the Ni^{++}. At 23°C the ratio of the rotational correlation time to that observed in aqueous standards $[\tau_c(\text{nerve})/\tau_c(H_2O)]$ was 3 on the basis of an exponential signal decay. Using this value and the Stokes' law relationship between viscosity and correlation time, this data indicates that most of the axoplasm has a microviscosity of 3 cp. Hypertonic solutions of 0.5 M $NiCl_2$ caused a several fold increase in microviscosity and hypotonic solutions of 0.05 M $NiCl_2$ a decrease. Disrupting nerve membranes by freezing and thawing or by glycercination significantly increased line widths, presumably by allowing Ni^{++} to enter the axoplasm. Supported by: PHS R01 NS 8706-06, and NSF GB 28664-X.

W-PM-B4 MICROSPECTROPHOTOMETRIC DETERMINATION OF IONIZED MAGNESIUM CONCENTRATION IN ISOLATED SQUID GIANT AXONS, A. Scarpa and F.J. Brinley Jr., Johnson Foundation, University of Pennsylvania, Philadelphia, Pa. 19174 and Dept. Physiology, Johns Hopkins Medical School, Baltimore, Md. 21205.

A technique has been developed for measuring ionized Mg^{++} concentrations in dialyzed squid giant axons. This technique is based on the microinjection of a metallochromic indicator for ionized Mg^{++} in the axoplasm of dialyzed giant squid axons and in the detection of its absorbance changes by sensitive dual wavelengths microspectrophotometry. The spectral characteristics of Eriochrome Blue SE (EB) allow for selections of λ pairs at which (Mg^{++}) can be measured at higher sensitivity without interference from (Ca^{++}) (Scarpa, Biochemistry 13, 1974, 2789). EB binds Mg^{++} very weakly (K_D= ~25 mM); it is scarcely bound to or has no side effects on functions of cells or subcellular organelles. The changes in absorbance of EB in the axoplasm were measured by focusing four time-shared monochromatic beams into a small area of the axoplasm with minute optical fibers and by recording the changes in absorbance of the dye at one isosbestic point and at the couple of λ pairs simultaneously. The axoplasm was then dialyzed with various concentrations of Mg^{++} through a porous dialysis capillary inserted longitudinally in the axoplasm (Brinley and Mullins, J. Gen. Physiol. 50, 1967,2303) and the intracellular concentration of free Mg^{++} in solution which produced no change in differential absorbance was noted. By this method, the ionized magnesium concentration in squid axoplasm was found to be between 3.0 and 3.5 mM. Hydrolysis of axoplasmic ATP induced by microinjection of apyrase produces kinetically measurable changes in differential absorption of EB, which are consistent with an increase in ionized (Mg^{++}) in squid axons. Supported by NS 08338, GM 12202 and HL 15835.

W-PM-B5 IMPLICATIONS OF NEGATIVE CHARGE DISTRIBUTION AT INNER SURFACE OF THE MEMBRANE. Gordon M. Schoepfle and Warren S. Rehm, Department of Physiology and Biophysics, University of Alabama Medical Center, Birmingham, Alabama 35294

In an attempt to account for shifts in the sodium inactivation curve associated with changes in internal ionic strength, Chandler, Hodgkin and Meves (J. Physiol. 180:821, 1965) proposed that fixed negative charges attached to the inner surface of the axonal membrane may generate a component of the electric field which can be altered by changes in ionic strength of the axoplasm. A decrease in the diffusion potential associated with sucrose replacement of internal KCl would then be offset by an increase in the field generated by the fixed charges. However, the mathematical analysis employed implies the assumption of a uniformly "smeared" layer of fixed charges on the surface of a cylinder which by the Gauss divergence theorem results in zero electric field within the enclosed volume. Hence there would exist no voltage difference between any two points in the axoplasm. These difficulties are obviated if it is assumed that the fixed negative charges are grouped in islands adjacent to sodium channels, some 1000 Å apart, at axoplasmic regions very near the membrane. Each island then acts as a separate center for a very nearly radial distribution of electric field in accordance with the Poisson-Boltzmann equation. This mechanism then provides the desired ionic strength dependent field across the membrane under conditions such that no voltage difference may exist between remote external fluid and center of axoplasm. (NIH 5P01-NS-08802, 2R01-EY00456 and NSF GBMS-72-02508).

W-PM-B6 EFFECT OF INTERNAL DIVALENT CATIONS ON SQUID AXON, D. C. Eaton and M. S. Brodwick*, Department of Physiology and Biophysics, University of Texas Medical Branch, Galveston, Texas 77550

Squid axons were perfused with low ionic strength solutions containing 20, 50, 100 and 200mM KCL and the I-V relationship recorded. Various concentrations (1, 5 or 20mM) of the alkaline earth cations were then added to the perfusate. Perfusion with any of these cations produced an alteration in the magnitudes of both the early inward current and the late outward current; however, the effectiveness of a particular cation in producing this change was often different depending upon which channel was examined. The order of the divalent cations effectiveness in reducing current in the early inward current pathway is $ca^{++}= Ba^{++}> Mg^{++}>Be^{++}$ (the position of Sr^{++} is not presently known) while the same sequence for the late outward channel is $Ba^{++}>>Sr^{++}=Ca^{++}=Mg>Be^{++}$. Generally the differences in effectiveness are not large with two exceptions: Ba^{++} is capable of totally blocking all of the late outward current at even the lowest concentrations applied. The rapidity with which it works suggest that much lower concentrations would be equally effective. Be^{++}, rather than causing a decrease in current, causes a 50 to 100% increase in current in both channels. Our results with Ca^{++} are contrary to previously published observations obtained with axons perfused with Ca^{++} at high ionic strength (Begenisich & Lynch, 1974). We feel that these differences may be explained by the differences in ionic strength since the alkaline earths seem to be more effective at the lowest ionic strengths studied.

W-PM-B7 STUDIES ON THE INTRACELLULAR pH OF SQUID GIANT AXONS. W.F. Boron* and P. De Weer, Department of Physiology and Biophysics, Washington University School of Medicine, St. Louis, Missouri, 63110.

The intracellular pH (pHi) of squid giant axons has been measured using glass micro-pH and membrane electrodes inserted through end cannulae into horizontally mounted axons. In artificial sea water (ASW, pH 7.6-7.8), pHi was 7.27 $\pm$ 0.02 (n=12). Application of external NH_4Cl caused a sharp increase in pHi, while return to normal ASW resulted in a fall of pHi to a value below the initial pHi. Prolonged exposure to NH_4Cl produced, after the initial rise, a slow decrease in pHi. Exposure of the axon to 5% CO_2, at constant external pH, caused a sharp decrease in pHi, which then (upon removal of the gas) returned to a value more alkaline than the initial one. Prolonged exposure of the axon to CO_2, however, resulted in (i) a slow increase in pHi after its rapid initial fall, and (ii) an exaggerated overshoot of pHi upon return to normal ASW. A mathematical model has been developed which describes variations in pHi as a function of the simultaneous passive flux of both the dissociated and the undissociated forms of a weak electrolyte. According to this model, the slow fall in pHi during prolonged exposure to NH_4Cl is caused by a continuous influx of NH_4^+ and a concurrent efflux of NH_3. The slow rise in pHi during chronic exposure to CO_2, as well as the overshoot occurring upon return to ASW, appear to require the operation of an active proton extrusion or sequestration mechanism.

Supported by NIH Training Grant # GM-02016 and NIH Grant # NS-11223.

W-PM-B8 EFFECT OF CYANIDE ON THE RESTING MEMBRANE POTENTIAL OF SQUID GIANT AXON. P. De Weer and D. Geduldig, Department of Physiology and Biophysics, Washington University School of Medicine, St. Louis, Missouri, 63110, and Department of Biophysics, University of Maryland School of Medicine, Baltimore, Maryland, 21201.

A small portion of the resting membrane potential of squid giant axon results directly from the operation of an electrogenic Na/K pump. Incipient cyanide poisoning, which is known to shift the pumping mechanism reversibly from Na:K exchange to Na:Na exchange, causes a slight membrane depolarization before any change in sodium efflux has occurred. This finding is compatible with the idea that Na:Na exchange through the sodium pump is non-electrogenic. Chronic exposure to cyanide, however, subsequently produces a sizeable (3 - 7 mV) hyperpolarization over a period of hours, during which time the membrane appears to become a better potassium electrode. Previous micro-injection of $CaCl_2$ (1 mM) into the axon has no effect on the magnitude of the CN-induced hyperpolarization; previous loading of the axoplasm with EGTA (10 mM) is similarly without effect on membrane hyperpolarization during prolonged CN poisoning. These data suggest that CN-induced hyperpolarization results from an increased membrane permeability to potassium, which is not mediated by high axoplasmic calcium levels. Intracellular pH undergoes acidification during CN poisoning, but this pH change can probably be ruled out as the cause for CN-induced hyperpolarization by the finding that axoplasmic acidification by CO_2 (at constant external pH) has little effect on membrane potential.

Supported by NIH grants #NS-11223 and #NS-08977.

W-PM-B9 FIXED CHARGES NEAR SODIUM AND POTASSIUM CHANNELS OF MYXICOLA AXONS. T. Begenisich* (Intr. by J.W. Prothero) Dept. Physiol. & Biophys., Univ. Wash. Sch. Med., Seattle, Wash. 98195

The effects of changes in the concentration of calcium in solutions bathing Myxicola giant axons on the voltage dependence of sodium and potassium conductance and on the instantaneous sodium and potassium current-voltage relations have been measured. The sodium conductance-voltage relation is shifted along the voltage axis by 13 mV in the hyperpolarizing direction for a four-fold decrease in calcium concentration. The potassium conductance-voltage relation is shifted only half as much as that for sodium. There is no effect on the shape of the sodium and potassium instantaneous current-voltage curves: the normal constant-field rectification of potassium currents is maintained and the normal linear relationship of sodium currents is maintained. Considering that shifts in conductances would reflect the presence of surface charges near the gating machinery and that shape changes of instantaneous current-voltage curves would reflect the presence of surface charges near the ionic pores, these results indicate a negative surface charge density of about 1 electronic charge per 120 A^2 near the sodium gating machinery, about 1e/300 A^2 for the potassium gating machinery and no surface charge near the sodium or potassium pores. There may be some specific binding of calcium to these surface charges with an upper limit on the binding constant of about 0.2 M^{-1}. The differences in surface charge density suggest a spatial separation for these four membrane components. Supported by PHS grant NS05846 and NSF grant GB24585.

W-PM-B10 URANYL ION BINDING TO AXONAL SURFACE CHARGES: EVIDENCE FOR PHOSPHATE STRUCTURE. J. D'Arrigo, Physiol. Dept, U of Utah, SLC, Ut 84132.

Previous work with crayfish axon (D'Arrigo, J. Physiol. 231:117, 1973; J. Physiol. (in press), 1974) has demonstrated the existence of clusters of surface acidic groups around the sodium gating structures. The actual local density of these surface negative charges at pH 7.0 has already been determined as close to that of certain types of phospholipid bilayers at about the same pH (D'Arrigo, 1973). From the above findings, one might hypothesize that most of these surface acidic sites represent phosphate groups of membrane phospholipids. To test this hypothesis, the effect of different extracellular alkaline-earth cations (Ca^{2+}, Mg^{2+}, Sr^{2+}, Ba^{2+}) upon the threshold membrane potential for spike initiation in crayfish axon has been studied by means of intracellular micro-electrodes. This was done at various extracellular concentrations of uranyl ion (UO_2^{2+}), which has been shown to bind exclusively to phosphate groups at concentrations below 10^{-5} M. At each concentration employed, extensive neutralization of axonal surface charges by UO_2^{2+} was evidenced by the fact that equal concentrations (50 mM) of alkaline-earth cations did not have the same effect on the threshold potential. The selectivity sequences observed at the different uranyl-ion concentrations were: 1.0×10^{-6} M UO_2^{2+}, $Ca^{2+} > Mg^{2+} > Sr^{2+} > Ba^{2+}$; 3.0×10^{-6} M UO_2^{2+}, $Ca^{2+} > Mg^{2+} > Ba^{2+} \geq Sr^{2+}$; 9.0×10^{-6} M UO_2^{2+}, $Ca^{2+} \approx Ba^{2+} > Sr^{2+} > Mg^{2+}$. These selectivity sequences are in accord with the equilibrium selectivity theory for alkaline-earth cations. At each of the concentrations used, uranyl ion did not have any detectable effect on the shape of the action potential itself. It is concluded that many (if not most) of the surface acidic groups in the region of the sodium gates represent phosphate groups of membrane phospholipids, but that the m gates themselves are probably proteinaceous in structure. (Sup: NIH Grant HL-16348.)

W-PM-B11 ION FLUX THROUGH SODIUM CHANNELS OF AXON MEMBRANE FRAGMENTS ISOLATED FROM LOBSTER NERVES. Raimundo Villegas, Flor V. Barnola*, and Paul Freund*, Centro de Biofísica y Bioquímica, Instituto Venezolano de Investigaciones Científicas (IVIC), Caracas, Venezuela.

The rate of sodium efflux, both in the presence and in the absence of drugs known to affect the passage of sodium ions through the axon membrane, was studied in vesicles formed by axolemma fragments isolated from lobster walking-leg nerves. The vesicles were suspended in lobster physiological solution containing 1 mM ouabain and equilibrated overnight with ^{22}Na added to the medium. Each preparation was divided into several portions: one for control, another to measure the effect of veratrine (0.5 mg/ml), and the other ones to study the effect of tetrodotoxin on the veratrine-treated vesicles. The vesicles were exposed to the drugs for three hours. Then the suspensions were diluted into nonradioactive solutions of the same composition and the ^{22}Na content of the vesicles as a function of time was followed by rapid filtration on Millipore filters. The results indicate that veratrine increases the ^{22}Na efflux rate from $5.9 \pm 0.4 \times 10^{-3}$ (mean ± SEM) to $8.6 \pm 0.5 \times 10^{-3}$ min^{-1}, while 10^{-7} M tetrodotoxin diminishes the increment of the ^{22}Na efflux rate from $8.6 \pm 0.5 \times 10^{-3}$ to $4.8 \pm 0.7 \times 10^{-3}$ min^{-1}. A 50% inhibition of the veratrine-increased sodium efflux occurs at a 12 ± 2 nM tetrodotoxin concentration. The measured dissociation constant of ^{3}H-tetrodotoxin to isolated axolemma preparations of lobster walking-leg nerves is 4.7 ± 0.9 nM. These findings suggest the presence of functioning sodium channels in the isolated fragments of axolemma.

W-PM-B12 TIME DEPENDENT VOLTAGE CLAMPS WITH AN OPEN SYSTEM TRANSPORT MODEL. Michael E. Starzak, State University of New York at Binghamton

An open system, sequential kinetic model of the form

$$\underset{4\beta}{\overset{g_K(V-V_K)}{\rightleftharpoons}} (1) \underset{3\beta}{\overset{\alpha}{\rightleftharpoons}} (2) \underset{2\beta}{\overset{2\alpha}{\rightleftharpoons}} (3) \underset{\beta}{\overset{3\alpha}{\rightleftharpoons}} (4) \xrightarrow{4\alpha}$$

generates approximate analytical solutions for current fluxes during time dependent voltage clamps. Since the sequential model reproduces the mathematical form of the Hodgkin-Huxley equations, these solutions provide insights into the function of such clamps. The approximate analytical solutions are

$$I_K = \bar{g}_K(V-V_K)[\alpha/(\alpha+\beta)]^4[1-\exp(-y(t))] \quad \text{with} \quad y(t) = \int[\alpha(t)+\beta(t)]dt$$

A steady state current-voltage relation for potassium currents is observed when the exponential decay term decays rapidly relative to the total period of the clamping waveform.

The basic analytical solutions suggest a technique for extracting rate constant data directly from pairs of time dependent clamps with different periods. The solutions also suggest that certain clamping waveforms will minimize the contribution of the exponential decay. The properties of a hyperbolic voltage clamp are examined in detail.

Supported by Grant R01-Ns-11676-01-PHY of the National Institutes of Health

W-PM-B13 CHLORIDE ACTIVITY IN THE GIANT CELL OF APLYSIA. Jeffrey D. Owen, H. Mack Brown and James H. Saunders, Department of Physiology, University of Utah College of Medicine, Salt Lake City, Utah 84132.

A large discrepancy in internal chloride activity (a^i_{Cl}) was observed in Aplysia giant cells when a^i_{Cl} was measured with Cl-sensitive liquid ion-exchanger or Ag/AgCl microelectrodes. The average value from 9 cells with the former was 38, whereas the latter yielded an average value of 152. This discrepancy was resolved by testing the selectivity of these two types of chloride electrodes to other anions. The Cl-selectivity of the ion-exchanger microelectrode is poor in HCO_3^-/Cl^- and Br^-/Cl^- solution mixtures, whereas the Cl-selectivity of the Ag/AgCl microelectrode is good in HCO_3^-/Cl^- mixtures but is extremely poor in Br^-/Cl^- solutions. A Ag/AgBr microelectrode with fair selectivity for bromide in Br^-/Cl^- solutions yields detectable bromide levels in the giant cell (approximately 1 mM). This is about the same amount of Br as there is in sea water (0.5 mM). The presence of Br^- in Aplysia giant cells would cause an overestimation of the amount of chloride present with both types of Cl electrodes. A corrected value for a^i_{Cl} taking Br in consideration is about 10 mM. The presence of a small amount of Br^- in squid giant axons might explain the discrepancy between the low chloride concentration measured by the Volhard titration technique (H. B. Steinbach, J. Cell. Comp. Physiol. 17, 57-64, 1941) and the high chloride activity measured with Ag/AgCl electrodes (R. D. Keynes, J. Physiol. 169, 690-705, 1963). This research was supported by USPHS Grant EY00762.

W-PM-C1 STAGEWISE BRAIN GROWTH IN MAMMALS. H.T.Epstein, Biology Dept., Brandeis University, Waltham, Massachusetts 02154.

Measurements of wet brain weight in mammals reveal periods of rapid increase occurring between periods of little or no increase. Data will be presented showing the growth periods in man, monkey, mouse, and rat. It will be indicated that the growth spurts are to be expected because of the special characteristics of brain growth, though the generality of the phenomenon is necessarily paralleled by a corresponding ignorance of what part or aspect of the brain is growing during any particular growth period. An additional significance of these periods derives from finding thresholds in behavioral development that occur in correlation with the brain growth periods. The evidence for these correlations will be given. The relationship of these findings to problems in human development will be briefly discussed.

W-PM-C2 THE EFFECT OF ETHYL NITROSO UREA (ENU), NERVE GROWTH FACTOR (NGF), AND ANTI-NGF ON NEURAL DIFFERENTIATION OF RAT PRIMARY CULTURES. S. Vinores* and J. R. Perez-Polo, Department of Zoology, University of Texas at Austin, Austin, Texas, 78712. (Intr. by A.R. Schrank).

ENU is a neurotrophic carcinogen when administered transplacentally to fetal rats. We wish to report that administration of ENU to primary cultures of fetal rat brain, cerebelum, spinal cord, and brachial plexus accelerates growth of these cells. NGF treatment increases neurite production. An intermediate response ensues when both NGF and ENU are administered transplacentally whereas treatment with anti-NGF accelerates cell division and markedly reduces neurite proliferation. Simultaneous exposure to anti-NGF and ENU gives a less dramatic response then anti NGF alone. Preincubation of ENU in rat liver homogenate has no effect. Neither the rat glioma cell line C6, nor the murine neuroblastoma cell line N2a responded to ENU or NGF at nontoxic levels. Supported by NINDS grant NS 11211 and BSSG grant from the University of Texas at Austin.

W-PM-C3 FUNCTIONS OF IMMATURE DENDRITES OF THE HYPOTHALAMIC RETICULAR ACTIVATING NEURONS OF NEWBORN. C.Torda. Mt.Sinai School of Medicine, N.Y., N.Y.,10029.

Scheibel, Davies & Scheibel(Exper.Neurol.,38,301,1973) have discovered that during the early postnatal period the dendrites of the reticular activating system have shaggy excrescences (heteromorphic protospines)(RAS). Within two months these spines disappear and excitatory and inhibitory synapses develop on the dendrites. Similar heteromorphic protospines have been found on the dendrites of the hypothalamic RAS of kittens. Through microelectrode measurements it has here been observed that these excrescences serve as postsynaptic membrane and are hypersensitive to stimuli and to neurotransmitters. They are able to generate spikes that may propagate. It seems that this system fulfills a very important physiological function: it generates crying, the only signaling system the newborn has to enlist the help of the mother to relieve his needs. In the newborn changes of the homeostatic equilibrium of several vegetative systems are communicated through changes of the physicochemical composition of the blood to neighboring nuclei of the hypothalamus (e.g. hunger, thirst, temperature and pressure changes).Activation of these nuclei excite the immature dendrites of nearby RAS neurons.The afferent neurons transmit these stimuli to the neocortex and the newborn awakens. The efferent neurons modify the respiratory rhythm in a manner to generate crying. This cry alerts the mother to provide relief for the arisen biological need. Maturation of RAS results in decreased sensitivity and increased specificity. Eventually, only very intensive stimuli(bordering on pain) will elicit crying.These results were obtained from newborn kittens by recording the activity of various RAS neurons by means of microelectrodes during stimulation of the various hypothalamic centers(or changes of physicochemical components of the blood).

W-PM-C4 SPREAD OF CURRENT FROM POINT SOURCES IN THE SPINAL CORD. C. Abzug *[1], The Rockefeller University, New York, NY 10021 and C.P. Bean, General Electric Company, Schenectady, NY 12301.

In connection with a study of the branching of vestibulo-spinal descending axons (Brain Research, 56 327-330) it became important to understand current spread from microstimulation electrodes placed at various points in the spinal cord. The principal factors influencing this spread, for a given electrode placement, are the geometries of the white and grey matter their relative electrical resistivities, and - especially for dorsal locations of the stimulating electrode - the existence of an insulating mineral oil pool above the cord. We have placed glass pipette or lacquer insulated tungsten electrodes at various locations in the white or grey matter of the spinal cord of the cat, in either the cervical or lumbar enlargement. Glass micropipettes were used to sense the local voltage pulses resulting from brief pulses of current flowing in the stimulating electrode from a remote indifferent electrode. Three major conclusions can be drawn from our experiments: first, we confirm the anisotropic nature of the electrical conduction process in the white matter (Exptl. Neurology, 11 451-463); second, we can identify the grey-white boundary through a characteristic change of local resistivity at the boundary; and finally, a simple model incorporating an electrical image of the stimulating electrode predicts the major effects of the mineral oil pool.

Supported in part by NIH Grant NS02619

1. Currently at U. of Md., School of Medicine, Baltimore, MD 21201
2. Guest Investigator, The Rockefeller University

W-PM-C5 STOCHASTIC SPATIOTEMPORAL CHARACTERIZATIONS OF MOUSE SPINAL SUBSTANTIAL GELATINOSA. G. L. Wilcox, Jr.* and M. W. Luttges, Aerospace Engineering Sciences, University of Colorado, Boulder, Colorado 80302.

The spatial-functional organization of the mouse spinal cord substantia gelatinosa was studied for afferent sensory barrages produced by sciatic nerve stimulation. Since many concepts of coding in the spinal cord depend upon the differential excitation of morphologically distinct populations of large and small cells, the ease with which such populations are functionally identified is of considerable interest. The spatial-temporal characteristics of multiple unit activity were analyzed stochastically for various types of afferent input. A functional characterization of mouse spinal substantia gelatinosa was achieved and a strategy for single electrode identification of statistically different populations of cells was developed.

The spinal cord of anesthetized (80 mg/kg, pentobarbital sodium) mice was exposed by laminectomy using a dissecting microscope. The sciatic nerve was also exposed and both exposures were covered with warm mineral oil. Spinal responses to sciatic nerve stimulation were recorded by two extracellular platinum microelectrodes (tip≈25μ). The electrode tips were separated by 150μ and each electrode was referenced to an indifferent electrode lodged in surrounding muscle. Two channels of unit responses were recorded simultaneously during stimulation. During the course of the observations, both electrodes were lowered systematically in 25μ steps. The data were analyzed into amplitude-discriminated, post-stimulus time histograms. These were used to construct cross-correlation coefficients for activity from both electrodes recorded throughout several penetrations of the substantia gelatinosa. Large cross-correlation values over large electrode displacements identified large cells. The strategy can be repeated using a single electrode at two different depths in the spinal cord.

W-PM-C6 TWO TYPES OF LGN CELLS. S.Hochstein and R.Shapley*, Rockefeller University, New York, N.Y. 10021.

Two main groups of ganglion cells - X and Y cells - send axons to the lateral geniculate nucleus of the cat. A temporally modulated spatial pattern can be positioned in the receptive field of an X-cell so as to produce no modulation of the cell's impulse rate, indicating linear spatial summation. Y ganglion cells have no null position due to nonlinear spatial summation. We now extend to the LGN this dichotomy. Extracellular recordings were made from LGN cells. The patterns used were sine gratings which were alternately introduced either (1) at a fixed contrast and then blanked or (2) at a positive and then negative contrast. Some geniculate cells have null positions. These are completely analogous to X retinal ganglion cells. For example, the figure shows PST histograms for such a cell when the grating was at the null position (lower) and at a quarter cycle away (upper). Stimulation here was type (2) 0.5 cps, 1.8 cycle/deg. We developed a quantitative specification of the strength of the null. Other geniculate cells analogous to retinal Y cells have no null position. Thus, the classification based on linearity of spatial interactions is as valid in the LGN as the retina.

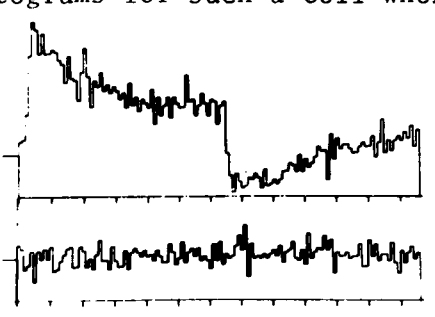

W-PM-C7 NEUROHYPOPHYSEAL PEPTIDES AND MEMORY. Josefa B. Flexner*, Louis B. Flexner*, Paula L. Hoffman* and Roderich Walter. Department of Anatomy, University of Pennsylvania, Philadelphia, Pa. 19104 and Department of Physiology, University of Illinois at the Medical Center, Chicago, Ill. 60612.

Increased attention is being focused on behavioral effects of brain peptides and their fragments. Lysine-vasopressin (LVP) and desglycinamide lysine-vasopressin (DGLVP) have been demonstrated both to facilitate acquisition of a conditioned avoidance response in hypophysectomized rats (Bohus et al., Neuroend. 11:137, 1973; Lande et al., J. Biol. Chem. 246: 2088, 1971) and to inhibit the extinction of such responses in intact rats (deWied, Nature 232:57, 1971; deWied et al., Br. J. Pharm. 45:118, 1972). In addition DGLVP can prevent the puromycin-induced blockade of expression of maze learning in mice (Lande et al., PNAS 69:558, 1972). Subcutaneous injection of mice with neurohypophyseal hormones and some of their analogs and fragments (0.1 mg in 15% gelatin) immediately after maze training, followed by bitemporal puromycin injection 24 hr after training, reveals that LVP, [tri-Gly]LVP, arginine vasopressin (AVP) and [1-deamino, 8-D-Arg]AVP confer a high degree of protection against the amnestic effects of puromycin. Synthetic DGLVP, 1-deamino-LVP, [4-Leu]LVP and H-Pro-Lys-Gly-NH_2 have moderately high activities, while H-Pro-Leu-Gly-NH_2 and H-Pro-Ile-Gly-NH_2 have relatively low activities. No activity was detectable with oxytocin, desglycinamide oxytocin, bovine neurophysin I and several other hormone fragments and analogs. The above results are discussed in terms of structure-activity relationships of the neurohypophyseal hormones and of known enzymatic inactivation patterns of these hormones.

Supported by NIH grant AM-18399 and NSF grant GB-42753.

W-PM-C8 NOREPINEPHRINE AND THE PATHOPHYSIOLOGY OF NEURONAL MEMBRANES. A. Bennun and S. Brydon Golz*, Department of Zoology and Physiology, Rutgers University, Newark, New Jersey 07102.

High levels of norepinephrine (NE) have been found in the urine of acute psychotic patients by William E. Bunney, Jr. Therefore, this study investigated the effects of NE on some properties of adenyl cyclase to elucidate the relationship between NE and the pathophysiology of membranes. Adenyl cyclase activity in rat cerebral cortex particulate preparations was measured by 3'5'cAMP production using a modification of the Gilman and Brown binding protein assays. Stimulation of adenyl cyclase by 1mM NE was maximal between the range of 0.025 to 0.25 mM ATP concentrations. The half maximal velocity ($K_{0.5}$) for ATP was 0.2mM and decreased to 0.07mM in the presence of 1mM NE. Preincubation of the particulate preparation for 3 hours with .1mM NE resulted in a 77% reduction in NE independent activity and loss of sensitivity to 0.1mM NE stimulation (NE desensitized). Preincubation for 3 hours with 5mM ATP or 5mM ATP-Mg resulted in a 2.98 to 3.6 fold increase in NE independent activity but desensitized the enzyme to 0.1mM NE stimulation. It is proposed that environmental conditions causing prolonged exposure to NE may alter the normal thresholds of adenyl cyclase response to hormones. This would result in abnormal levels of cAMP, preventing proper cell function.

W-PM-C9 ASSOCIATION OF GLUTAMIC ACID WITH GRANULE CELLS IN THE CEREBELLUM. W.J. McBride*, K. Kusano* and M.H. Aprison, Depts. of Psychiatry and Biochemistry and the Institute of Psychiatric Research, Indiana University Medical Center, Indianapolis, Ind. 46202 and Dept. of Biology, Illinois Institute of Technology, Chicago, Ill. 61606.

The putative amino acid neurotransmitters glutamic acid, aspartic acid, GABA and glycine, as well as alanine, were assayed in the cerebrum, brain stem (including the diencephalon) and cerebellum of mice with neurological mutations of the 'staggerer' or 'weaver' type. In both types of mutants there is an almost complete absence of granule cells in the cerebellar cortex. In the cerebellum of the staggerer mutant: (a) the content of glutamate decreased to a value of 6.62 ± 0.70 from 12.0 ± 0.49 μmoles/g tissue wet wt. ($P < 0.005$); (b) the content of glycine and alanine was higher in the case of the staggerer mutant than in controls; and (c) there was no difference in the levels of aspartate and GABA between normals and the staggerer mutants. In the cerebellum of the weaver mutants: (a) the content of glutamate decreased to 8.77 ± 0.76 from 12.0 ± 1.3 μmoles/g tissue wet wt. ($P < 0.025$); (b) the content of GABA and glycine was significantly greater than normal levels, and (c) there was no difference in the levels of alanine and aspartate between the two groups of mice. The content of these 5 amino acids was the same in the cerebrum and brain stem of the staggerer mutants, weaver mutant and the corresponding control group. These data are in agreement with the findings of Young et al. (Brain Res. 23: 1, 1974), who reported a selective depletion of glutamic acid was associated with a viral induced granule cell loss in hamster cerebellum, and support the suggestion that glutamic acid may be the excitatory transmitter released from the cerebellar granule cell. (Supported in part by NIMH Grant 03225-16)

W-PM-C10 PURIFIED MAMMALIAN BRAIN ACETYLCHOLINESTERASE-A GLYCOPROTEIN. Eugene Gardner, Sin-Lam Chan,* Don Thorne, Jr.*, and Anthony J. Trevor,* Department of Pharmacology, University of California at San Francisco, San Francisco, California 94143

Acetylcholinesterase is a membrane bound enzyme with important functions in central cholinergic transmission. We have documented the presence of carbohydrate moieties in enzyme isolated from bovine caudate nucleus tissue. Their functional significance is, as yet, unknown. The enzyme is purified by affinity and molecular sieve chromatography evidencing multiple molecular forms. Polyacrylamide gel electrophoresis on a micro-scale was used to verify the purity and homogeneity of the preparation in a quantifiable manner. Protein standards establish the limits of sensitivity of the gels at the 20 ng level. Thus, 1 μg of sample can verify 98% purity. Similarly, one can demonstrate the carbohydrate components using the periodic acid-Schiff technique. The limit of detection here is at the 30 ng level. Electrophoresis is followed by fixation with trichloracetic acid, oxidation with periodic acid, and treatment with Schiff reagent to develop the glycoprotein bands. Protein is detected with Coomassie blue dye and activity bands are developed by incubation in a buffered substrate-tetrazolium dye medium. The specific reversible binding of the enzyme to a sepharose-conconavalin A column provides additional evidence for the presence of glycoside. Both crude and relatively pure preparations show a high degree of binding and elution with a recovery of 75-80% and a 10-15 fold increase in specific activity.

W-PM-C11 INTERACTION OF CHLORPROMAZINE WITH BRAIN MICROTUBULE SUBUNIT PROTEIN. Norman D. Hinman* and John R. Cann, Biophysics and Genetics Department, University of Colorado Medical Center, Denver, Colorado 80220

We have found that the psychoactive drug chlorpromazine (CPZ) at concentrations of 10^{-5} to 10^{-3}M interacts reversibly with brain microtubule subunit protein (tubulin) in vitro and in so doing inhibits the rate of reassembly of microtubules and the binding of colchicine by the protein. It also causes disassembly of microtubules formed in the absence of the drug. Control experiments with trimethylamine and ethyldimethylamine demonstrate that the inhibitory action of CPZ specifically involves the phenothiazine moiety and is not due simply to the binding of a tertiary amine. Although the degree to which CPZ inhibits colchicine binding is independent of the colchicine concentration over the range, 10^{-6} to 10^{-3}M, CPZ does cause partial reversal of the binding of colchicine. These results are most easily explained formally in terms of a noncompetitive interaction. Hill plots for CPZ-inhibition of reassembly and colchicine binding in an imidazole buffer system, pH 6.8, suggest that CPZ binds to 2 or more sites in a moderately cooperative fashion. Further analysis utilizing the statistical mechanical Ising model of nearest neighbor interaction supports this interpretation. In contrast, the Hill plot for inhibition of colchicine binding in a phosphate buffer system, pH 7.5, indicates that CPZ acts by binding to 1 or more independent sites. An explanation for this apparent buffer effect awaits the outcome of direct binding studies now in progress. Supported in part by Research Grant 5R01 HL 13909-23 from the NIH.

W-PM-C12 A REGIONALLY LINEAR MODEL OF NEURON INTERACTION. Belmont G. Farley, Dept. of Computer and Information Sciences, Temple Univ., Philadelphia, Pa. 19122.[1]

This paper discusses systems of interacting neurons having the following general model properties: (1) Neurons are represented by their membrane voltage in one or more compartments; (2) interaction between compartments is by linear electrotonus or synaptic "excitation"; (3) Interaction produced by action potentials is represented by excitation which is a function of average impulse rate; (4) the effect of synaptic excitation is to produce a membrane voltage rate-of-change proportional to the value of the incoming excitation; (5) Excitation outgoing from a compartment is a fixed linear function of membrane voltage between certain voltage thresholds. Upon crossing such a threshold, the linear function may change. This model leads to a system of non-linear differential-difference equations whose variables are the membrane voltages of compartments. Behavior, however, is linear within the regions of the variable-space bounded by the membrane voltage thresholds, so that linear solutions can be "patched" together at these boundaries. Since the interaction between neurons is represented by continuous functions, the model applies, within its approximations, to neural interaction with or without "action potentials." Analytic and computer studies show that particular model systems can: (1) Simulate any logical function; (2) Support controlled wave propagation in both linear and non-linear modes; (3) Produce a variety of controlled, time-dependent, parallel outputs, as in motor behavior; (4) Respond decisively to classes of time-dependent, parallel inputs, as in recognition behavior; (5) "Record" impressed inputs for a period of time, as in short-term memory.

[1]Supported by Temple University and NIH FR-15

W-PM-D1 NANOSECOND SPECTROSCOPY OF FLUORESCENT RESIDUES BOUND TO NATURAL AND ARTIFICIAL MEMBRANES. W. X. Balcavage* and T. Alvager,* Indiana University School of Medicine, Indiana State University, Terre Haute, Indiana 47809. (Intr. by J. Swez)

Nanosecond fluorescence decay spectroscopy has been applied to an examination of tryptophane residues in pure proteins, and in proteins embedded in natural and artificial membranes. It has been shown that the lifetime of the fluorescent event is highly pH sensitive and critically dependent upon the wavelength of the exciting light and the dielectric nature of the environment of the tryptophane moiteies. These properties have been useful in determining the distribution of tryptophane residues in quiescent biomembrane systems and isolated mitochondrial membrane proteins. The fluorescence quantum yield of proteins and membranes contained in reaction systems with variable quantities of fluorescence quenching material, eg., OH^-, H_2O , suggest that only a small proportion of tryptophane residues is accessible to aqueous environments and it is proposed that the unequal distribution of tryptophane residues in aqueous and nonaqueous environments may be used to follow membrane and membrane protein conformation changes which are related to physiological functions.

W-PM-D2 PHOTO-ELECTRIC EFFECTS IN BILAYER LIPID MEMBRANES WITH ABSORBED CYANINE DYES. Jay S. Huebner, Department of Natural Sciences, University of North Florida, Jacksonville, Florida 32216.

The voltage waveforms resulting from an 8 μsec light flash are reported for ten structurally distinct cyanine dyes absorbed to one side of BLM of lecithin and oxidized cholesterol. Two types of waveforms are observed, which correlate with features of the dye structures. Three dyes induce a fast effect (F) in which the voltage rises in ~100 μsec and returns to the baseline in ~0.5 sec, in BLM with resistance-capacitance (RC) times of ~5 sec. Five dyes reduce the BLM resistance, create an offset voltage, and induce a slow effect (S) which rise in ~5 sec in BLM with RC times of ~5 msec. F dyes, such as 3,3' dimethyl 2,2' oxacarbocyanine iodide and 3,3' diethyl 2,2' thiacarbocyanine iodide, have mirror symmetry about the vinylene chain, and two exposed oxygen or sulfur atoms. S dyes, such as 1,1' diethyl 2,2' cyanine iodide and 1,3' diethyl 4,2' quinolylthiacyanine iodide, have at least one quinoline ring and require iodide to induce S. Two dyes, 3,3' diethyl 2,2' oxathiacarbocyanine iodide (which lacks mirror symmetry) and 3,3' diethyl 9 ethyl 2,2' oxacarbocyanine iodide (which has an ethyl group covering its oxygen atoms), don't induce any photo-voltages, both dyes lacking quinoline rings. F is argued to be generated by a photo-polarization and orientation of dye molecules in the membrane/aqueous interface. Their relaxation discharges the voltage in less than the BLM RC time. S is believed to result from a photo-chemical reaction disturbing the diffusion equilibrium of the dye and iodide across the BLM. F amplitude increases linearly with the light intensity; S amplitude increases with the square of the light intensity.

W-PM-D3 OXIDATION KINETICS OF REDUCED RIBOFLAVIN-5'-MONOPHOSPHATE VIA O_2 AND BACTERIAL LUCIFERASE USING A COMPUTER CONTROLLED RAPID SCANNING STOPPED-FLOW SPECTROMETER. George J. Faini, Richard J. DeSa* and John Lee, Department of Biochemistry, University of Georgia, Athens, Ga. 30602

A NOVA mini-computer equipped with a general purpose interface has been utilized to control data acquisition generated by a kinetic spectrometer. A standard, commercially available, monochromator has been modified and coupled with a Durham stopped-flow instrument to provide absorption spectra with a maximum range of 500 nm at a rate of 100 spectra/second. A brief description of the hardware and the computer program will be presented. Using this spectrometer, the auto-oxidation of riboflavin-5'-monophosphate (FMN) at pH 7, 5°C, has been observed for wavelengths 320 to 570 nm over a 5 second time interval with spectra measured at 100/second. One millisecond time resolution was obtained at several fixed wavelengths of special interest. The FMN was purified by ion-exchange chromatography. Flavin was photoreduced and maintained anaerobic prior to mixing. Kinetic absorption spectra have also been measured under the same conditions for the oxidation of $FMNH_2$ by two types of the bacterial luciferase. With concentrated, highly active, luciferase, auto-oxidation is negligible and a biphasic oxidation has been observed which entails several enzyme intermediates. In contrast, under these conditions, auto-oxidation of $FMNH_2$ exhibits precise isobestic points and therefore proceeds with no detectable intermediates. This work is supported by grants from NIH (GM19163-01A1 and GM16834-06) and Public Health Research grant GM02619-01 (to G.J.F.) from the National Institute for General Medical Sciences.

W-PM-D4 THE PHOTOPROTEIN CHROMOPHORE OF AEQUORIN AND MNEMIOPSIN: ITS IDENTITY WITH RENILLA LUCIFERIN. W.W. Ward*, K. Hori* and M.J. Cormier* (Intr. by J.K. Zimmerman), Bioluminescence Laboratory, Department of Biochemistry, University of Georgia, Athens, Georgia 30602.

The bioluminescent systems of the jellyfish Aequorea and the ctenophore Mnemiopsis have been isolated and purified as protein-chromophore complexes. These photoproteins (aequorin and mnemiopsin) produce light in an oxygen-independent intramolecular reaction initiated by calcium ions (Shimomura et al., 1974, Biochemistry 13, 3279; Ward and Seliger, 1974, Biochemistry 13, 1491 & 1500). The oxygen-dependent light-producing system of the sea pansy Renilla, however, requires the participation of two organic components luciferin and luciferase (Hori et al., 1973, Biochemistry 12, 4463). Previously published indirect evidence (Cormier et al., 1974, Biochim. Biophys. Acta 346, 137) concluded that photoproteins may contain a Renilla-like luciferin. To account for the oxygen independence of photoproteins, a protein-stabilized luciferin hydroperoxide has been proposed. Absorption spectra of native aequorin and mnemiopsin resemble the absorption spectra of Renilla luciferin in aprotic and protic solvents respectively. The isolated product of the aequorin reaction, Aequorea oxyluciferin, is chemically and spectrally similar to Renilla oxyluciferin, and the etioluciferins are identical. Finally, the storage form of Renilla luciferin, luciferyl sulfate, has been isolated from tissue extracts of both Aequorea and Mnemiopsis. We will present direct evidence that the chromophore of aequorin and mnemiopsin is in fact Renilla luciferin and, furthermore, that the protein-bound chromophore exists as luciferin rather than as the luciferin hydroperoxide. We propose the general term "coelenterate luciferin" to describe the light-producing chromophores from all such bioluminescent coelenterates.

W-PM-D5 SPECTRAL AND PHOTOCHEMICAL CHARACTERIZATION OF A REDUCED FLAVIN-LIKE CHROMOPHORE ASSOCIATED WITH BACTERIAL PHOTOEXCITABLE LUCIFERASE. S.-C. Tu* (Intr. by M.Z. Nicoli), The Biological Laboratories, Harvard University, Cambridge, Mass. 02138.

Bacterial bioluminescence in vitro normally occurs when bacterial luciferase reacts with reduced flavin mononucleotide ($FMNH_2$), molecular oxygen, and a long chain aldehyde. Extracts of luminous bacteria also contain "photoexcitable luciferase", a modified luciferase molecule which is inactive in the chemically initiated reaction, but is active photochemically. In the absence of added FMN or $FMNH_2$, flash irradiation of the photoexcitable luciferase initiates light emission which qualitatively resembles the $FMNH_2$-dependent bioluminescence. It has been shown that photoexcitable luciferase is a complex protein involving a chromophore (designated B) tightly associated with luciferase. The protein-bound B exhibits a single absorption peak (λ_{max} about 375 nm) in the near-ultraviolet to visible region. The bound B is fluorescent, with an excitation maximum at 375 nm and an emission maximum at 495 nm. Free B, however, is nonfluorescent in aqueous solution at room temperature. Repeated flash irradiation of the luciferase:B complex in the presence of oxygen progressively converts B to FMN as identified spectrally, enzymatically, and chromatographically. These spectral and photochemical findings lead to the hypothesis that B is a 4a-substituted FMN. A mechanism for the photoexcited bioluminescence reaction is also suggested. (Supported by NSF grant EMS74-23651 and NIH grant GM 19536)

W-PM-D6 FLUORESCENCE AND BIOLUMINESCENCE OF THE OXYGENATED BACTERIAL LUCIFERASE-FLAVIN INTERMEDIATE ISOLATED BY LOW-TEMPERATURE CHROMATOGRAPHY. C. Balny* and J.W. Hastings, Institut de Biologie Physico-Chimique, 13 rue Pierre et Marie Curie, Paris 5 France, INSERM, U 128, BP 5051, Montpellier, France, and the Biological Laboratories, Harvard University, Cambridge, Mass. 02138.

Bacterial luciferase ($\alpha\beta$ dimer, M.W. 79,000) catalyzes the oxidation of reduced flavin mononucleotide ($FMNH_2$) by molecular oxygen; long chain aldehyde is required for bioluminescence but not for the formation of a long lived oxygenated intermediate. This intermediate has been isolated in pure form by Sephadex chromatography at -20°, and maintained and studied at -20° to -30°. The intermediate has an absorption peaking at about 372 nm and a relatively weak fluorescence excited at this wavelength. The fluorescence emission is in the 480 to 520 nm range, apparently involving more than one species. Upon continued exposure of the intermediate(s) to light, the intensity of the fluorescence increases by a factor of 5 or more and its spectrum shifts to that of an apparently single component with an emission maximum at about 485 nm (uncorrected for phototube sensitivity). Upon warming, this fluorescence is lost and the fluorescence of oxidized flavin mononucleotide (FMN) appears; if warming is carried out in the presence of a long chain aldehyde, bioluminescence occurs during the transition. The emission spectrum of the bioluminescence, peaking at 485 nm, corresponds exactly to the fluorescence emission spectrum of the intermediate formed by irradiation, suggesting that the latter may be structurally similar to the emitting species in bacterial bioluminescence. (Supported by NSF grant EMS74-23651)

W-PM-D7 N- AND C- TERMINAL AMINO ACID SEQUENCES OF THE SUBUNITS OF BACTERIAL LUCIFERASE. T.O. Baldwin, M.Z. Nicoli, D.A. Powers* and J.W. Hastings, The Biological Laboratories, Harvard University, Cambridge, Mass. and Dept. of Biology, The Johns Hopkins University, Baltimore, Md.

The luciferases from two species of luminous marine bacteria, believed to be representative of two distinct groups, have previously been isolated and characterized. The enzymes from both species (Beneckea harveyi [Bh] and Photobacterium fischeri [Pf]) are heterodimers consisting of two nonidentical subunits, α and β (Biochemistry 8, 4681 [1969]). Although both subunits are required for activity, they have been shown to be functionally distinct in that the catalytic center appears to reside on the α subunit (Biochemistry 10, 4069 [1971]; Biochemistry 11, 3359 [1972]). Tentative sequences have now been established for the N-termini of the α and β subunits of the luciferases from both species:

Bh α MKFGNFLLTYQPXELSQTEVMKALVN Pf α MKFGNISFSYQPSGE
Bh β MKFGLFFLNFMNSKXSXDQVLEEMXN Pf β MKFGLFFLNFQKDGI

Positions marked X were not determined unambiguously. Preliminary amino acid sequence analysis of the C-termini indicates that this region is also very similar in all four polypeptide chains. These amino acid sequence similarities imply not only that the Pf and Bh luciferases are homologous (Biochemistry 9, 4949 [1970]), but that the α and β subunits have arisen by a gene duplication, presumably prior to divergence of the lines leading to present-day luminous bacteria. Amino acid sequence similarity implies three-dimensional structure similarity; this possibility is of obvious importance in view of the functional dissimilarity between the subunits and the evidence for a single flavin binding site per αβ dimer (J. Biol. Chem. 246, 7666 [1971]; B.B.R.C. 57, 1000 [1974]).

W-PM-D8 ANAEROBIC BACTERIAL LUCIFERASE SYNTHESIS. Anatol Eberhard* (Intr. by H. A. Scheraga), Department of Chemistry, Ithaca College, Ithaca, New York 14850.

The luciferase content of luminous bacteria grown under totally anaerobic conditions in the presence of sodium dithionite was investigated. Luciferase was assayed semi-quantitatively by aerating the anaerobic cultures and measuring the light emitted by the bacteria in vivo. The bacteria emit no light at all when growing anaerobically. After several anaerobic serial transfers, aeration produced a large amount of light, showing that luciferase synthesis had occurred during anaerobic growth. These findings suggest that luciferase may have some role other than that of light production.

W-PM-D9 LIGHT EMISSION BY LUMINOUS BACTERIA IN THE OPEN OCEAN. C. R. BOOTH* and K. H. NEALSON* (Intr. by J. E. Becvar) Scripps Institution of Oceanography, La Jolla, Cal. 92037.

The model of autoinduction of bacterial bioluminescence proposed by Nealson, Platt, and Hastings (J. Bact. 104:313,1970) makes the interesting prediction that free floating luminous bacteria will be inactive in light emission. Using low light level measuring techniques we have studied the luminescence of bacteria in the open ocean. Sea water samples were first passed through 10 μ filters to remove larger organisms, then measured for luminescent activity with a high resolution photomultiplier and appropriate amplification. Samples were routinely either devoid of bioluminescence or exhibited extremely low levels. These samples were then filtered on 0.2 μ nucleopore filters, and the filters incubated at ambient sea water temperature on sea water agar plates. By this method the number of viable luminous bacteria which were present in the measured samples was determined. The luminous colonies were then purified and pure cultures examined for luminescence after dilution into sterile sea water. By this method it was found that the luminescence of single cells could be easily measured. From this information we have concluded that the luminous bacteria found floating free in sea water are either completely inactive or are emitting light at levels far below their potential. Similar experiments were performed at many localities, depths, and times of day, and though the concentration of luminous bacteria per ml of sea water fluctuated over a 10 fold range, there was never a correlation between the number of luminous bacteria and the amount of light per sample, and the cells were always found to be extremely inefficient in bioluminescence.

W-PM-D10 HYDROSTATIC PRESSURE EFFECTS ON THE CONTROL OF BIOLUMINESCENCE IN GONYAULAX. V.D. Gooch and W. Vidaver*, Department of Biological Sciences, Simon Fraser University, Burnaby, British Columbia, and The Biological Laboratories, Harvard University, Cambridge, Mass. 02138.

Gonyaulax polyedra, a marine dinoflagellate, spontaneously luminesces in two kinetic forms: a) as a flash with a decay half time on the order of 100 msec., and b) as a continuous low level glow. Cellular control for bioluminescence is evident since Gonyaulax has a far greater capacity for bioluminescence than it shows spontaneously. A step application of hydrostatic pressure to any value in the range of 350 to 800 atm. initiates increased bioluminescence displayed as at least three distinct kinetic forms: a) the rate of flashing increases, b) the glow intensity increases to a maximum at about 5 sec., and c) the glow again increases to give a second peak at about 1 min. For a given higher initial step in pressure, there is an increased rate and magnitude of flashing, and the glow peaks are larger and reached faster. When the pressure is released there is an immediate large intensity glow which rapidly decays, often with biphasic character. Most aspects of the glow phenomenon can be modeled by considering two systems each having a pair of sequential first order reactions in which an increase of pressure causes the rate of the first reaction to be greatly increased and the rate of the second to be decreased. An investigation of the in vitro reaction between the soluble luciferin and luciferase always showed an increase in intensity with increased pressure. The magnitude of this pressure effect strongly depends upon the pH and the form of Gonyaulax luciferase which is used.

W-PM-D11 OXYGEN AND THE ULTRAWEAK CHEMILUMINESCENCE OF BIOMEMBRANES OF THE RAT. Jerzy W. Meduski*, Bernard C. Abbott, S. C. Wen*, Jerzy D. Meduski*, and Glen Hoshizaki*. USC, Dept. of Biol. Sci. and Dept. of Physiology, Los Angeles, CA 90007.

Addition of ferrous ions to the preparations of rat cytomembranes (microsomes or mitochondria) in a medium composed of KCl (35 mM), $MgCl_2$ (30 mM), sucrose (0.25 M), and K_2HPO_4/KH_2PO_4 buffer (0.05 M, pH 7.4) triggers three concomitant events: oxygen uptake by the preparation, increase of its lipid peroxide content and the outburst of ultraweak chemiluminescence. The peak of the chemiluminescence coincides with the cessation of the increase of lipid peroxides and with the cessation of oxygen uptake. Light emission responses of mitochondria of liver, brain, kidney, heart, skeletal muscle or lung of the rat (decreasing sequence) are proportional to the ability of the mitochondrial preparations from corresponding organs to take up oxygen under these conditions. This oxygen uptake is directly proportional to the ability of a cytomembrane system to form lipid peroxides, and inversely related to the venous pO_2 of the same organ. Our results lend support to the concept that the reversible binding of molecular oxygen by a cytomembrane system of an organ acts as an intracellular regulatory mechanism of oxygen uptake by this organ.

(Supported by the Allan Hancock Foundation and an HEW grant HL 12556).

W-PM-E1 ELECTROPHYSIOLOGICAL EFFECTS OF APRINDINE: ALTERATIONS OF CALCIUM-DEPENDENT MEMBRANE PROCESSES. Joseph Reiser* and Alan R. Freeman. Dept. of Physiology, Temple Univ. School of Medicine, Phila., Pa. 19140.

Superfusion of isolated canine Purkinje fibers with APRINDINE (APR) [N-phenyl-N(3-diethylamino propyl)-2-indamylamine HCL] reveals an antidysrhythmic action. Observed are decreases in conduction velocity, refractoriness and rate of rise of phase 0 as well as an associated depression of phase 4 depolarization in spontaneous fibers. An initial effect of APR involved a striking decrease in action potential duration due to a distinct abolition of phase 2 (action potential plateau) while steady state membrane properties were minimally altered. The present study was undertaken to attempt to account for such observations. In Tyrodes solution containing normal concentrations of calcium (Ca^{++}), exposure of doubly impaled surface cells to APR (10^{-5}M) resulted in a decreased effective membrane resistance (R_{eff}) to 72% of control values with little change in Resting Potential. Subsequent evaluation of R_{eff} in high Ca^{++} medium (8.1,16.2mM) however revealed a considerable reduction in the effectiveness of APR. Furthermore, decreasing Ca^{++} levels to 1 and 0.1mM, also lessened the influence of APR on membrane resistance. Propagated action potentials obtained in sodium free, Ca^{++}-rich solutions simulating a form of the tissue's slow response were distinctly inhibited by APR, further substantiating its Ca^{++} involvement. The above findings indicate that antidysrhythmic effects of APR may involve Ca^{++} mediated mechanisms. Although these findings relate to primary involvements of Ca^{++} mediated membrane phenomena, effects of APR involving the rate of depolarization of the action potential do exist, which may add in part toward the effective nature of this agent when compared to commonly employed anti-dysrhythmic agents such as lidocaine.

W-PM-E2 REACTIONS OF L-CELLS TO PENETRATION BY HAMSTER SPERMS. L. C. Lau, Department of Botany, University of Toronto, Toronto 5, Ontario, Canada. Intr. by A. M. Rauth.

Epididymal sperms from Syrian golden hamster were combined with mouse L-cells under standard conditions of tissue culture with 0.5% fructose added to enhance sperm motility. Gentle mixing was provided by a roller tube for 24 hours, after which the admixture was allowed to attach and grow on microscopic slides for examination. Separate cultures of sperms and L-cell were maintained as controls. Cells penetrated by sperms became polynucleated with time. These cells in turn broke up to give rise to a population morphologically distinct from those not treated with sperms. Further incubation saw the generation of globules by these transformed cells of one or more nuclei. Appearing in the cytoplasm in varying number, these spherical structures are of uniform size and seemed to be released into the vicinity of the cell. Depending on the conditions of cell culture and the growth state of L-cells before mixing, it takes about three weeks for the admixture to attain globule-bearing stage. Together with the host nuclei, many of the globules stain positively in DNA-specific dyes. Barring unforseen contamination, the consistant reproducibility of the observation and its absence from separate cultures of sperms and L-cells suggest that some manner of transformation and replication may have taken place within L-cells by hamster sperms. (Supported by the National Cancer Institute of Canada)

W-PM-E3 IMAGING WHOLE CELLS BY HVEM AND STEM. Norman C. Lyon* (SPONSOR: J. Turner) Roswell Park Memorial Institute, Buffalo, New York 14203.

Developments in high voltage electron microscope (HVEM) and transmission scanning electron microscopy (STEM) have spawned techniques that require increased penetrability by the electron beam. Stereo-imaging is one such case. More significant is the development of hydration chambers (EMC's) to view wet biological specimens and hopefully living cells. Concurrent studies in our laboratory include development of EMC's for both the HVEM and STEM. A comparison of the imaging of critically point dried (CPD) mammalian cells (mouse fibroblast-3T3, L-929 & Ehrlich ascites tumor) on an AEI 1 MeV HVEM and STEM on an adapted Philips EM-300 at 60KV is reported. Cells grown on Formvar/carbon coated gold grids were fixed in 4% glutaraldehyde at 37°C, dehydrated through alcohol, and CPD from Freon 113. Cells examined at 1 MeV showed sufficient nuclear penetration to reveal the nuclear membrane enclosing chromatin bodies. Cytoplasmic organelles e.g. mitochondria were clearly visible, with excellent imaging of cell peripheries showing microvilli and blebs. In STEM cells were visualized on the CRT of a Philips scanning unit and recorded as polaroid prints. STEM showed comparable penetration of cell nuclei with well-defined nuclear membranes and nucleoli. Cytoplasmic detail including vacuoles and intracellular granules were clearly visible, although the recording process reduces image quality. The dynamic range of grey levels produced required at least two exposures to encompass all the information. Improved amplification with adequate filtering (homomorphic) would help correct this. Parallel processing should enhance the image but not to the clarity obtained with HVEM. Modified STEM could prove a cheaper way of obtaining increased penetrability for examining wet biological samples in an EMC. Our laboratory is currently exploring this possibility. (Supported by NIH GM-16454)

W-PM-E4 DNA, PROTEIN, AND NUCLEAR AND CYTOPLASMIC DIAMETER MEASUREMENT IN MAMMALIAN CELLS. J. Steinkamp* and H. Crissman,* Biophysics and Instrumentation Group, Los Alamos Scientific Laboratory, University of California, Los Alamos, New Mexico 87544.

A new technique for rapid and simultaneous measurement of total DNA and protein and nuclear and cytoplasmic diameters in single cells has been developed. This method is based on quantitative fluorescent staining of cells for DNA with mithramycin or for both DNA and protein with propidium iodide (PI) and fluorescein isothiocyanate (FITC) which fluoresces red and green, respectively. Depending on which staining procedure is used, two methods of cell analysis are possible. Cells stained with a fluorescent dye(s) enter a flow chamber and flow at a constant velocity across a narrow shaped argon laser beam of exciting light, causing fluorescence and light-scatter signals to be generated. Electronic integration of the red and green fluorescence signals gives total DNA and protein on PI/FITC-stained cells. Similarly, total fluorescence and light-scatter signals yield DNA content and whole cell size from mithramycin-stained cells. The time duration of these signals also can be electronically measured and converted into signals proportional to nuclear and cytoplasmic diameter. The above cellular parameters can then be processed singly or as ratios and displayed as frequency distribution histograms. The basic principles of this new methodology will be discussed with specific application to mammalian cell systems. (This work was performed under auspices of the U. S. Atomic Energy Commission and the National Cancer Institute.)

W-PM-E5 BABOON CELL SYSTEMS FOR ENVIRONMENTAL HAZARD DETERMINATION I. ALVEOLAR MACROPHAGES.

M. L. Meltz, E. M. Gause*, and J. R. Rowlands*, Department of Environmental Sciences, Southwest Foundation for Research and Education, San Antonio, Texas 78284.

The functional role of the alveolar macrophage involves the clearance of particulate matter from the lung, and requires phagocytic action by these cells. While particles so ingested are located in phagosomes, and presumably are subsequently secreted from the cell, many questions remain as to what may happen to any hazardous chemicals initially bound to the particles. These chemicals can be eluted and/or metabolized by enzymes once inside the phagosome. If such chemicals are released into the macrophage, they can interfere with its functional ability, or kill the cell. One possibility is that the DNA of the cell will be damaged. Repair replication is well documented in human and rodent cells. Since this process is associated with the repair of ultraviolet light and chemical induced damage of DNA, we propose to use measurement of such repair as an indicator of macrophage DNA damage. We have determined that repair does occur in alveolar macrophages of the baboon obtained by lung lavage after exposure to ultraviolet light, and will report on results obtained after treatment with MMS, a direct alkylating agent, and benz(α)pyrene, which must be metabolized to an active form. We will also report on the presence of aryl hydrocarbon hydroxylase activity in the baboon macrophage, since such activity would be involved in the metabolic alteration of chemicals to a form which can damage DNA.

W-PM-E6 THE DEVELOPMENT OF THE AMAC TRANSDUCERS AND HISTOCHEMISTRIES FOR THE DETERMINATION OF ATYPICAL EXFOLIATED CELLS.

R.C. Leif, R.A. Thomas, B.F. Cameron, H.G. Gratzner, V. Powers, D.J. Ingram, S.P. Clay, and S.B. Leif, Papanicolaou Cancer Research Institute, P.O. Box 6188, Miami, Florida 33123.

A new combined potential sensing electronic cell volume and optical transducer, the AMAC IV, has been constructed and is undergoing testing. The problem of performing combined fluorescence and light scattering has been solved by utilizing a water immersion microscope objective. The water immersion lens lies approximately 1 mm from the stream and does not disturb the flow of the cell containing stream. Since the windows are at comparatively great distance from the stream, precise light scattering studies are feasible. The technology to fabricate another type of transducer with a square orifice out of quartz, the AMAC III, has been developed and a complete unit will soon be fabricated. An optical system including electronic shield for the pulsed laser compatable with both AMAC transducers has been developed. A computer system which is upwardly compatable for multidimensional analyses has been extensively utilized for electronic cell volume analysis with the AMAC II laminar flow potential sensing electronic cell volume transducer. This system is capable of obtaining spectra at 250,000 cells per min. The resolution of the electronic cell volume spectra is considerably improved of other nonlaminar flow systems. Specific antibody against 5 BrdU has been produced and will serve as a useful descriptor of DNA synthesis. Centrifugal Cytology is now being utilized to monitor agents for the dissociation of exfoliated cervical cells. Supported by NIH Grants #RO1-CA-13441 and GM-1867 and NCI Contract #NO1-CB-43962.

W-PM-E7 INFLUENCE OF LIMITATIONS OF OXYGEN DIFFUSION ON CELL SURVIVAL IN AN IN VITRO MODEL SYSTEM.

A. Franko*and R. Sutherland*, (Intr. by M.R. Roach), Ontario Cancer Treatment and Research Foundation, Victoria Hospital and Department of Biophysics, University of Western Ontario, London, Ontario, Canada.

An in vitro model has been developed which permits study of the effects of diffusion limitations of metabolites on the properties of cells in a tissue-like environment. Chinese hamster V79-171b lung cells in suspension grow as multicellular spheroids which can attain 700 μm diameters. They develop central necrosis, with a viable outer rim of cells of approximately 200 μm thickness containing an inner shell of non-cycling, hypoxic cells. They are considered to be models of solid tumors which have similar tissue organization and develop chronically hypoxic cells which are resistant to treatment with radiation. Spheroids were grown in a complete nutrient medium in various oxygen tensions (.02% to 20%). The thicknesses of viable rims of cells as determined from measurements of histological sections agreed with predictions of diffusion theory for oxygen. Unknown factors other than oxygen influenced the viable rim thickness at oxygen concentrations less than 2%. The length of time cells were able to survive when beyond the oxygen diffusion limit was determined by abruptly shifting spheroids to extremely low oxygen tension (200 ppm) and then monitoring the development of necrosis histologically and the viability of cells from spheroids by colony formation. Correlation of the histological and viability data indicates that different cell populations die at different rates.

Supported by Grant #227, Ontario Cancer Treatment and Research Foundation and a Medical Research Council Studentship.

W-PM-E8 APOCYTOCHROME C OXIDASE IN COPPER DEFICIENT YEAST CELLS.

Ezzatollah Keyhani and Jacqueline Keyhani*, Johnson Res. Fdn., U. of Penn., Philadelphia, Pa. 19174, and Molecular Biology Inst., Brussels, Belgium.

When yeast is grown in a copper deficient medium, cytochrome c oxidase cannot be detected spectrophotometrically (FEBS Letters, 17, 127, 1971). By use of double labeling techniques employing ^{14}C or ^{3}H labeled leucine in copper deficient and copper containing medium, respectively, it is possible to demonstrate that the six polypeptides of cytochrome c oxidase are synthesized in copper deficient cells. The apparent molecular weights of these polypeptides are: 45,000, 34,000, 24,000, 17,500, 12,000 and 9,000 daltons, respectively. The reconstitution kinetics of cytochrome c oxidase in copper deficient cells grown in copper supplemented medium suggests that an active process is involved in the transport of copper within the cell. The reconstitution of the active cytochrome c oxidase does not occur in the presence of cycloheximide, an inhibitor of cytoplasmic protein synthesis, whereas it does in the presence of inhibitors of mitochondrial transcription (ethidium bromide) or translation (chloramphenicol). In the case of the inhibitors of mitochondrial protein synthesis, however, the reconstitution of cytochrome c oxidase representes 25% of the untreated cells. This value is due to the presence of the apoprotein in copper deficient cells, before de Novo synthesis of cytochrome c oxidase becomes inhibited. Therefore we conclude: 1)in copper deficient cells, the apoprotein part of cytochrome c oxidase is synthesized and integrated into the mitochondrial membrane; 2)a cytoplasmic copper protein exists and is involved in the transport and/or integration of the copper into the apoprotein moiety of cytochrome c oxidase; 3)the incorporation of copper into the apoprotein restores the catalytic function of the active enzyme, since copper deficiency does not alter the heme synthesis (Proc.Soc.Exptl.Biol.Med. 127,977, 1968).

W-PM-E9 BIOGENESIS OF MITOCHONDRIA IN THE SLIME MOLD, DICTYOSTELIUM DISCOIDEUM, DURING RECOVERY FROM ETHIDIUM BROMIDE TREATMENT. L. Kobilinsky*, R.N. Stuchell*, B.I. Weinstein* and D.S. Beattie, Department of Biochemistry, Mount Sinai Schoolof Medicine, New York, New York 10029.

After addition of ethidium bromide (EB) to cultures of slime mold amoebae, cell growth continued for 1 or 2 more generations. The specific activity of cytochrome oxidase in whole cells started to decrease immediately after addition of EB, while that of succinate-cytochrome c reductase decreased more slowly. By contrast, the specific activity of succinate dehydrogenase (SDH) increased nearly 2-fold in cells treated with EB for 5 days. In purified mitochondria from EB-treated cells, the content of cytochromes a-a_3 was decreased over 80% and that of cytochrome b nearly 50% compared to control mitochondria. The specific activity of SDH, however, was identical in mitochondria from control and EB-treated cells suggesting that continued formation of new mitochondria with an identical complement of SDH must occur despite the cessation of cell growth. Electron micrographs indicate that gross changes in the mitochondrial cristae have occurred after growth in EB for 5 days. Upon removal of EB from the medium, the cells immediately resumed growth, the cytochrome a-a_3 content increased reaching control values within 4 generations, and the specific activity of SDH in whole cells gradually decreased reaching control levels after 5 generations. Possible controls for the formation of the mitochondrial membrane will be discussed. (NIH grant HD-04007).

W-PM-E10 A MOLECULAR WEIGHT STUDY OF HUMAN FIBROBLAST INTERFERON. F. H. Reynolds, Jr.* and Paula M. Pitha, The Johns Hopkins University School of Medicine, Oncology Center, Baltimore, Maryland 21205.

Electrophoresis of unpurified human fibroblast interferon in polyacrylamide gels containing urea, sodium dodecyl sulfate and 2-mercaptoethanol resulted in only one biologically active peak of 25,000 daltons. The interferon was eluted from the gels in phosphate buffered saline (0.14 M NaCl and 0.02 M phosphate buffer, pH 7.4). Renaturation of the interferon was accomplished in the presence of 50% fetal bovine serum upon dilution into Eagle's minimal essential medium. Interferon was assayed by inhibition of the cytopathological effects of vesicular stomatitis virus. Electrophoresis of human interferon in the absence of urea resulted in multiple fractions with interferon activity. This is interpreted as aggregation of interferon with impurities; thus explaining the confusing multiple molecular weights previously reported. Coomasie blue stained gels of unpurified interferon showed only high molecular weight bands (60,000 to 100,000). Not only do these data establish the molecular weight of human fibroblast interferon, but also point out that human fibroblast interferon probably exists in nature, predominantly as a complex with serum proteins. (This work was supported by grants from NIH [AI 10944-03] and American Cancer Society, Md. Divn. [74-24].)

W-PM-E11 THE ROLE OF PARTICLE SIZE AND CHARGE IN THE CLEARANCE OF LIPOSOME ENCAPSULATED DRUGS. D. Stamp* and R. L. Juliano, Research Institute, Hospital for Sick Children, Toronto, Canada.

Lipid microvesicles (liposomes) containing trapped drugs or enzymes have been suggested as useful tools in cancer chemotherapy and in the amelioration of enzymatic deficiencies. Here we report on the effect of particle size and surface charge on the clearance of liposomes from the rat bloodstream. By varying the time of sonication during vesicle preparation, either multilamellar or paucilamellar liposome can be generated. The multilamellar samples elute entirely in the void volume of Sepharose 4-B columns, while the paucilamellar samples are entirely retarded. The surface charge of phosphatidyl choline/cholesterol vesicles can be modified by the addition of phosphatidyl serine (negative charge) or stearylamine (positive charge). Multilamellar vesicles are cleared from the circulation more rapidly than paucilamellar ones. Thus the intial clearance rate (expressed at $t_{\frac{1}{2}}$) of paucilamellar phosphatidyl choline/cholesterol vesicles was 22 minutes, as opposed to 6 minutes for the multilamellar variety. Likewise surface charge affects clearance rates; the $t_{\frac{1}{2}}$ for intial clearance of neutral, positive, and negative paucilamellar vesicles was 22 min, 20 min and 6 min respectively. We also show that encapsulation of chemotheraputic drugs results in a substantial modification of their clearance rates.

This study was supported by the National Cancer Institute of Canada.

W-PM-E12 EFFECTS OF ULTRAVIOLET IRRADIATION ON BEATING OF EMBRYONIC CHICK HEART CELL AGGREGATES. Richard D. Nathan, John P. Pooler, and Robert L. DeHaan, Departments of Anatomy and Physiology, Emory University, Atlanta, Georgia 30322.

Heart cell aggregates were irradiated with ultraviolet light at wavelengths between 260 and 310 nm. The characteristic light-induced effect was an initial increase in beat rate to a maximum plateau level, followed by an abrupt cessation of beating. The action spectrum for the time to termination of beating peaked between 290 and 295 nm; it fell off sharply at longer wavelengths and more slowly at shorter wavelengths. This action spectrum agreed qualitatively with spectra reported recently for the UV-induced reduction in sodium current recorded under voltage clamp conditions for frog nodes of Ranvier (J.M. Fox, Pflüg. Arch. Ges. Physiol. In press) and lobster giant axons (G.S. Oxford and J.P. Pooler, J. Mem. Biol. In press). In contrast the maximum change in beat rate was increasingly greater for shorter wavelengths and exhibited no peak in the wavelength range investigated. The UV sensitivity of aggregates, as measured by the inverse of the irradiation time required to terminate beating, decreased with increasing aggregate size and external potassium concentration, was relatively independent of temperature, and increased with embryonic age.

Supported by USPHS grants HL 16567 and NS 09040.

W-PM-E13 ULTRASONIC EFFECTS ON MELANOMA CELLS IN CULTURE. E. Armour*, P. Corry, and J. McGinness*, Department of Physics, M.D. Anderson Hospital & Tumor Institute of The University of Texas System Cancer Center, Houston Texas 77025.

We have demonstrated that the pigment melanin is an amorphous semiconductor and that the pigment behaves as a threshold switch. Based on these observations we have proposed that the biological role of the melanin is to behave as a nonlinear energy transduction device, behaving as a protective device or a cytotoxic agent depending on the mode and level of input of energy in the form of environmental agents. Experiments have been carried out to test this proposal. The experimental results indicate that pigmented cells (human malignant melanoma) are preferentially killed relative to nonpigmented cells in culture by 10KHz and 1MHz ultrasonic radiation. Studies on DNA strand scission (alkaline sucrose density gradients) also demonstrated that DNA damage is greatly elevated in pigment containing cells by ultrasonics, presumably due to creation of long lived free radicals.

This research was supported in part by AEC contract AT-(40-1)-2832 and grant CA05099 from the Public Health Service.

W-PM-E14 PURIFICATION AND BIOPHYSICAL CHARACTERIZATION OF RABBIT GLOBIN AND SILK-MOTH CHORION PROTEIN MESSENGER RNA. J. N. Vournakis, Department of Biology, Syracuse University, Syracuse, New York 13210; and A. E. Efstratiadis* and F. C. Kafatos*, Department of Biology, Harvard University, Cambridge, Massachusetts 01238.

Studies on the purification and characterization of two classes of eukaryotic mRNA are described. Magnesium precipitation of polysomes, phenol extraction, sucrose gradient and polyacrylamide/formamide gel electrophoresis techniques for purifying mRNA are used. A new assay for the purity of poly(A) containing RNA is discussed as applied to these mRNAs. The method utilizes the polynucleotide phosphorylase phosphorolysis enzymatic activity, and PEI-cellulose thin layer chromatography. The assay has been designed to be rapid so that routine measurements of mRNA purity are possible. A series of biochemical and biophysical studies with the two mRNAs are discussed, including composition analysis and optical rotatory dispersion measurements. Preliminary conclusions concerning secondary structural properties of the mRNAs are presented.

W-PM-F1 LIGHT-DRIVEN LEUCINE TRANSPORT IN HALOBACTERIUM HALOBIUM CELL ENVELOPE VESICLES. R. E. MacDonald* and J. K. Lanyi, Biological Adaptation Branch, NASA-Ames Research Center, Moffett Field, CA 94035.

H. halobium cell envelope preparations containing bacteriorhodopsin eject protons on illumination and take up C^{14}-leucine, against up to a 1000-fold gradient. After illumination the leucine is lost rapidly and exponentially. Na^+ in the medium is absolutely required and K^+ inside the vesicle greatly enhances uptake. FCCP abolishes both H^+ efflux and leucine influx; membrane-permeant cations leave H^+ efflux unchanged but greatly reduce leucine influx, and nigericin in the presence of K^+ decreases the net H^+ efflux without affecting leucine influx. Valinomycin (in the presence of K^+) and gramicidin D inhibit leucine uptake, while arsenate and DCCD have little effect. When a Na^+ pulse was added to vesicles devoid of internal Na^+, transient uptake of leucine was observed in the dark. The above results suggest that leucine is carried into the cell envelope vesicles together with Na^+, in response to a negative potential created by the bacteriorhodopsin-mediated H^+ efflux.

W-PM-F2 EFFECTS OF LIGHT PERTURBATION ON THE ABSORPTION SPECTRA OF PURPLE MEMBRANE FROM HALOBACTERIA HALOBIUM. Brian M. Becher and Joseph Y. Cassim, Department of Biophysics, The Ohio State University, Columbus, Ohio 43210.

Purple membrane from Halobacteria halobium R_1 was isolated and purified as previously reported (Fed.Proc.33 1408, 1974)[1]. The following features are observed in the absorption spectra of the purple membrane in buffer (pH 7): (1) A major chromophoric band at 559 nm. (2) Minor bands at 412, 390, 372, 340, and 324 nm with approximately 0.25 times the intensity of the 559 nm band. (3) Several overlapping protein aromatic π-π^* bands with maxima at 290, 280, and 274 nm which have 1.3, 1.7, and 1.67 times the 559 nm band intensity, respectively. (4) A shoulder at 223 nm arising from the protein amide n-π^* transition. With light perturbation the following changes in the absorption spectra are observed: (1) The 559 nm band shifts to 567 nm and increases in intensity by 12%. (2) The minor bands in the spectral region 450-300 nm undergo 1 to 10% changes in intensity and red shift from 2 to 12 nm. (3) The 290, 280, and 274 nm bands undergo 1% increases in intensity with no shift in band positions. However, no change is observed in the 223 nm shoulder. Evidence from the above absorption studies suggest that light perturbation affects the chromophoric transitions indicating a change in the transition environment. However, the fact that this perturbation has little effect on the protein transitions may be interpreted as indicative of the protein conformation undergoing no significant global changes with illumination. These results are in agreement with circular dichroic spectra studies of light-perturbed purple membrane.

W-PM-F3 EFFECTS OF LIGHT PERTURBATION ON THE CIRCULAR DICHROISM OF PURPLE MEMBRANE FROM HALOBACTERIA HALOBIUM. Brian M. Becher and Joseph Y. Cassim, Department of Biophysics, The Ohio State University, Columbus, Ohio 43210.

Purple membrane from Halobacteria halobium R_1 was isolated and purified as previously reported (Fed.Proc.33 1408, 1974). The following features are observed in the circular dichroic (CD) spectra of the purple membrane in buffer (pH 7): (1) Negative and positive extrema at 595 and 525 nm respectively with the crossover at 563 nm. The 595 nm band has 0.8 times the intensity of the 525 nm band. (2) A negative extremum at 318 nm with 1.6 times the intensity of the 525 nm band. (3) Several overlapping CD bands in the 300-250 nm spectral range arising from the protein aromatic π-π^* transition. The major feature in this region is a positive extremum at 263 nm with 0.8 times the intensity of the 525 nm band. (4) Two negative extrema at 209 and 222 nm arising from the π-π^* and n-π^* amide transitions of the protein, respectively. The ellipticity of the 222 nm band suggests a protein helical content of approximately 45%. With light perturbation the following changes are observed: (1) The 595 and 525 nm extrema shift to 602 and 538 nm respectively with 25% increases in intensity. The 563 nm crossover shifts to 574 nm. (2) The 318 nm extremum increases 25% in intensity with no shift. However, no observable changes occur in the 300-250 nm region or in the 222 and 209 nm extrema. These results support the suggestion from the absorption spectra studies that light perturbation does not result in the significant global changes in the protein conformation. However, it is clear that the asymmetric environment of the chromophore is altered by light perturbation. The unique profile of the visible CD and its correlation to the 559 nm absorption band suggests exciton interaction. It's also possible to explain this spectral phenomena by evoking an ad hoc existence of a unique combination of bands.

W-PM-F4 LOW TEMPERATURE KINETICS OF H^+ CHANGES OF BACTERIAL RHODOPSIN. B. Chance, M. Porte*, B. Hess* and D. Oesterhelt*. Johnson Fdn., Univ. Penna., Phila. PA 19174; Max-Planck-Inst. Dortmund and Munich Univ., Munich, Germany.

Low temperature photolysis with fast fluorometric readout has been developed for a more precise evaluation of the kinetics of H^+ release in suspensions of purple membrane patches from Halobacterium halobium ($\sim$90 µM rhodopsin) (Oesterhelt & Hess, Eur. J. Biochem. 37:316,1973) in salt solutions diluted with $\sim$25% ethylene glycol, F.P. $\sim$-40°. Photolysis is activated by a liquid dye laser emitting 1 µsec light pulses at 585 nm. Two pH indicators are used: 9 - 30 µM 4-methyl umbelliferon (UBF; 366 nm excitation, 450 nm emission) and 15 µM carbazine-122 (Eastman Kodak)(620 nm excitation, 680 nm emission) covering the pH range from 6.2 to 8.0. In the temperature span from -28° to -40° in the liquid phase, the half-time for H^+ release increased from 25 to 100 msec. Simultaneous dual wavelength spectrophotometry at 640-700 nm and 550-540 nm showed no correlation with intermediates prior to R_4 (DeVault et al., These Abstracts) and a good correlation with the $R_3 \rightarrow R_4$ kinetics for both H^+ release and uptake. Cooling to below the freezing point did not substantially alter the reaction kinetics as extrapolated from the liquid state, nor was a significant rate change observed within the range of the two pH indicators. Controls were afforded by light activation of the reaction outside the range of the indicators; very small changes were observed below -50°, presumably due to the accumulation of intermediates prior to R_4. Thus the H^+ release is clearly identified with a dark reaction of $k = 30\ sec^{-1}$ at -28° and a high energy of activation, the fourth step of the sequence observed by DeVault et al.

Support from USPHS GM 12202 and the Max-Planck Gesellschaft.

W-PM-F5 PHOTOLYSIS OF BACTERIAL RHODOPSIN. D. DeVault, M. Chu Kung*, B. Hess* and D. Oesterhelt*. Johnson Fdn., Univ. Pennsylvania, Phila. PA 19174 Max Planck Inst., Dortmund and Univ. Munich, Munich, Germany.

Suspensions in aqueous salt solution of purple membrane of *Halobacterium halobium* Mutant NRL R_1M_1(1,2) were photolyzed with 20 ns pulses at 539 nm. The initial material R_0 shows peak absorption, A, at 568 nm(2). Four successive products, R_1-R_4, were observed at -25°($(CH_2OH)_2$ added). $R_0 \rightarrow R_1$ occurs in <1μs with quantum efficiency near 1. ΔA is a bleaching thruout the visible region. 90-95% of ΔA reverts in ∿ 10μs signalling a corresponding loss of efficiency for forming R_2 to R_4, compared to a high efficiency of R_4 formation at room temp(2). R_2 is formed during the decay of R_1, $t_{1/2} \leq$ 10 μs. Depending on the state of the sample, R_1 and R_2 are not always resolved. Relative to R_0, ΔA peaks at 650-680 nm. R_2 forms with $t_{1/2}$∿20-100 μs as shown by disappearance of most of the A at 650 nm. R_4, the product studied in (2), forms with a $t_{1/2}$∿16 ms; its spectrum relative to R_0 has peaks at 412 and 680 nm. R_1 appears to be an excited state, possibly triplet, preceding isomerization which seems hindered at low temp. R_2,probably all-trans, may correspond to pre-lumi-R in the visual case (3). Both are strongly red-shifted from R_0. R_3 may be an unresolved mixture and could correspond to lumi-R and meta-R-I. R_4 would then correspond to meta-R-II. Both are strongly blue-shifted from R_0 and their formation involves H^+: release in bacteria(4) and uptake in vision. Bacterial rhodopsin recycles repeatedly even at -25°. R_4 returns directly to R_0(2) so it is probable that retinal does not separate from the protein. At room temp we seem to have the same succession of products with rates speeded. $R_2 \rightarrow R_4$ is 35 μs at +25° and 500 μs at 0°. (Support from PHS GM 12202 and NSF GB 26700).
1)Oesterhelt & Stoeckenius, Nature NB 233:149,1971;2)Oesterhelt & Hess, Eur J. Biochem.,37:316,1973;3)Wald, Nature 219:800,1968;4)Chance et al These Abs.

W-PM-F6 A SPIN LABEL STUDY OF PURPLE MEMBRANES FROM *Halobacterium halobium*. C.F. Chignell and D.A. Chignell*, National Heart and Lung Institute, Bethesda, Maryland 20014 and Department of Biochemistry, University of Dundee, Scotland.

The isolation of a purple-colored fragment from the cell membrane of the extreme halophile *H. halobium* represents one of the first successful attempts to obtain a simple membrane system capable of translocating hydrogen ions (PNAS 70: 2853, 1974). Purple membrane (PM) contains a single protein, bacteriorhodopsin, which constitutes about 75% of its dry weight. In contrast to the mammalian visual receptor membrane, PM phospholipid side chains are highly saturated, consisting of dihydrophytol groups linked to phosphatidylglycerol by ether linkages (Biochemistry 5: 4092, 1966). We have probed the molecular organization of PM with the aid of N-oxyl-4',4'-dimethyloxazolidine derivatives of 5-ketostearic acid (I), 12-ketostearic acid (II) and 16-ketostearic acid (III). Labels I and II exhibited maximum hyperfine splittings ($2T_m$) of 62 G and 60.7 G when bound to PM at 25°. An Arrhenius plot of $2T_m$ for I bound to PM showed a single discontinuity at 29° which was abolished when the PM were crosslinked with glutaraldehyde. PM crosslinked with glutaraldehyde also showed a small but significant decrease in rigidity. The ESR spectrum of III bound to PM revealed the presence of two populations of bound spin label, one of which was highly immobilized. These studies suggest that PM are extremely rigid structures in which a large proportion of the lipid is present as boundary lipid closely associated with bacteriorhodopsin.

W-PM-F7 LIGHT-DEPENDENT CHANGES IN ELECTRICAL POTENTIAL OF CELL ENVELOPE VESICLES FROM HALOBACTERIUM HALOBIUM MEASURED WITH A CYANINE DYE.
R. Renthal and J.K. Lanyi, NASA-Ames Research Center, Moffett Field, Cal.

Upon illumination, the purple membrane photoreceptor protein of Halobacterium halobium, bacteriorhodopsin, cyclically passes through a series of photointermediates. The net result of a single photoreaction cycle is the uptake of one proton inside the cell and the release of one proton outside the cell per mole of bacteriorhodopsin. Vesicles prepared from sonicated cell envelopes of H. halobium contain oriented patches of purple membrane, and proton translocation has been observed in vesicles as well as in cells. We have investigated the electrical potential across envelope vesicle membranes resulting from this proton efflux.

The cyanine dye di0-C_5-(3), when added to a suspension of vesicles, shows a light-dependent decrease in fluorescence emission of up to 35%. This decrease is maximal at dye concentrations of 5×10^{-7} M, vesicle protein concentrations of 0.35 mg/ml, pH 6.0, and in NaCl. In KCl, the decrease is less than half as much. The fluorescence decrease is linear with incident light intensity up to about 6×10^5 ergs/cm^2/sec. The rate of decrease is nearly identical to the rate of proton efflux. When the light is turned off, the rates of return of pH and fluorescence are also the same. In NaCl, triphenylmethylphosphonium ion abolishes the fluorescence decrease but enhances the proton efflux. We conclude that the observed fluorescence changes detect electrical potential across the vesicle membrane.

(R.R. is a NRC Resident Research Associate.)

W-PM-F8 USE OF GUANIDINE AS A PROBE ION FOR THE DETERMINATION OF THE MITOCHONDRIAL MEMBRANE POTENTIAL. J. Fields* and B.C. Pressman, Department of Pharmacology, University of Miami, Miami, Florida 33152.

Mitochondrial (M) membrane potentials were determined from the distribution ratios of subinhibitory concentrations of guanidine (G) and its derivatives between rat liver M and incubation medium. Accumulation of ^{14}C-G was measured by counting the medium and M following separation by centrifugation or millipore filtration. If the entire accumulation of G in the M after ½ hr equilibration in State 4 is divided by the matrix volume, the $[G]_{in}/[G]_{out}$ is ∿10 over a wide range of [G]. This sets an upper limit of -60 mV as the maximum negativity of the M interior; if an appreciable fraction of accumulated G resides in the membrane rather than in the matrix as assumed in the calculation, the potential would be more positive. By two phase distribution G is ∿15 fold more lipophilic than K^+ indicating its likely equilibration across the M membrane within the test period. The [G] in the medium following removal of M by centrifugation sets limits on the membrane potential consistent with the millipore technique. When these experiments were repeated with more lipophilic probes (hexyl-G, octyl-G), increasingly higher limits were obtained reflecting increased probe accumulation within the M membrane (-111mV, -154mV). Even though alkyl-G accumulation occurred largely within the membrane phase, it was nevertheless controlled by the metabolic state of the M, State 4>State 3>State 3U, hence metabolic control of cation accumulation by M need not be mediated by the membrane potential. The same factors governing accumulation within the membrane also explain the apparent energy dependency of the inhibition of electron transport in M by G and its derivatives. These results appear inconsistent with the large membrane potentials required by the chemiosmotic mechanism of M energy transduction.

W-PM-F9 4-WAVELENGTH SPECTROPHOTOMETRY OF CYTOCHROMES IN BULL-FROG GASTRIC MUCOSA. G. W. Kidder III, Dept. of Physiology, Univ. of Maryland Sch. of Dentistry, Baltimore, MD 21201

The dual-wavelength spectrophotometer has been modified to alternate between two wavelength pairs on a 1 minute cycle. Using this instrument, it is possible to observe 2 cytochrome signals at the same time, providing better kinetic correlations than previously available. In 10% CO_2/90% O_2, the initial steady state of cytochrome c in stimulated tissue was 68% reduced (0% = SCN inhibited, 100% = anoxic). This is larger than the values previously reported in 5% CO_2. Cytochrome b and cytochrome a(+a_3) were less reduced in comparison. A surprising finding was that flavoprotein (fp) did not show changes in optical density between aerobic and anaerobic conditions, implying that its steady state is 100% reduced. All cytochromes (but not fp) showed an overshoot upon reoxygenation, with a time course similar to that of cytochrome c, but with a generally smaller magnitude relative to their total concentration. The peak of the overshoot is roughly coincident with the resumption of acid secretion and the peak in the potential difference record. All cytochromes are oxidized by 10 mM NaSCN. Changing the mucosal solution from pH 3.5 to as low as pH 1.0, which Hersey has reported (BBA 334:157) to produce a crossover between fp and cytochrome c, had no effect on either component, although conventional overshoot and SCN-oxidation persisted at acid pH. We thus fail to confirm the exciting finding of Hersey. The reasons for this failure are not yet evident. (Supported by NSF GB-36278)

W-PM-F10 THERMODYNAMICS AND KINETICS OF MODEL PHOTOSYNTHETIC REACTION CENTERS. R. J. Anderson* and R. T. Ross, Department of Biophysics, The Ohio State University, 484 W. 12th Avenue, Columbus, Ohio 43210

Photosynthetic quantum conversion, modeled as a Markov process, is simulated on a digital computer to determine what thermodynamic losses are a necessary consequence of specific assumptions about reactions along a chain of molecules. The behavior of model systems with one primary acceptor is comparatively independent of whether thereis one or an infinite number of molecules that can donate electrons to the reaction center, and whether there is one or an infinite number of secondary electron acceptors. Maximal free-energy yield requires that all forward rate constants be at least 10^2 times the rate of light absorption, and that all reverse rate constants be at least the rate of light absorption. Maximal yield also requires that all dark reactions be in near equilibrium, so the potential of all half-cells on the donor side of the light act is the same, and the potential of all half-cells on the acceptor side is the same. A system having no triplet state can convert light energy with a nearly ideal efficiency, provided that the midpoint potentials of the reaction center and the primary acceptor half-cells are precisely located with respect to one another and to the potentials of the donor and acceptor pools. While not necessary for near maximal free-energy yield, a triplet or other metastable intermediate of the reaction center allows a flexibility in the choice of half cell potentials which is not possible in the absence of such an intermediate. For systems, either with or without a triplet intermediate, having a single donor to the reaction center, the standard potential of the half-cell for the donor can vary widely without substantially hurting the free-energy yield. (NSF GB-35503)

W-PM-F11 EFFECT OF COUNTER ANION ON THE OXIDATION OF N-BENZYL-1, 4-DIHYDRONICOTINAMIDE. P. E. Blatz and H. Kawashima*, Department of Chemistry, University of Missouri-Kansas City, Kansas City, Missouri 64110.

The oxidation of N-benzyl-1,4-dihydronicotinamide, and NADH model compound, by malachite green has been studied. The reaction rate was found to be dependent on the kind of malachite green salt employed. The bimolecular rate constants were obtained for the chloride, bromide and iodide, and the following ordering was obtained: $k_{Cl} > k_{Br} > k_I$. Activation parameters for the reactions were obtained.

Results of these experiments could indicate that the distance of the negative charge from the nitrogen determines the electron distribution or polarization of the aromatic ring. In an enzyme this mechanism could control the reversibility of $NAD^+ \rightleftarrows$ NADH reactions.

W-PM-F12 THE INITIAL PHASE OF THE SARCOTUBULAR ATPase REACTION. D. C. Pang* and F. N. Briggs, Department of Physiology, Medical College of Virginia, Virginia Commonwealth University, Richmond, Virginia 23298.

Analysis of the initial phase of the calcium stimulated, magnesium dependent ATPase activity of rabbit skeletal sarcoplasmic reticulum (SR) was undertaken with the aid of β,γ-methylene 8-^{3}H ATP. Since ATP was found to be a competitive antagonist to the binding of the analogue, the analogue and ATP apparently bind to the same site. Scatchard analysis of the analogue binding data, obtained in the presence of 5 mM EDTA, indicates that there are approximately 4 nmoles of a single class of sites per mg SR protein and that the dissociation constant of the analogue for this site is 1.7×10^{-5} M. Binding of the analogue was found to be competitively inhibited by magnesium, if calcium was excluded by addition of 5 mM EGTA. The K_I for Mg was 5×10^{-4} M. Analogue binding was inhibited by low ($<5 \times 10^{-4}$ M) concentrations of calcium. Since low concentrations of calcium stimulate the rate of EP formation and we have found calcium to inhibit ATP binding, the effect of calcium on the rate of EP formation must be a step beyond substrate binding.

W-PM-G1 QUASIELASTIC LASER LIGHT SCATTERING STUDIES OF TROPOELASTIN COACERVATION. by A. M. Jamieson and K. Tansey*, Department of Macromolecular Science, Case Western Reserve University, Cleveland, Ohio 44106†.

The coacervation behaviour of tropoelastin†† is a phase separation with an upper consolute temperature which has the features of a mixed coacervation (1) and seems to be driven by both simple (non polar) and complex (electrostatic) interactions. We report quasielastic light scattering studies of a coacervating tropoelastin system which suggest that coacervation of dilute tropoelastin solutions occurs because of a positive configurational entropy change due to randomization of the protein chain segments in the coacervate. We conclude that the phase separation involves a transition from 'ordered' (micellar) aggregates in the dilute phase to independent random coils in the coacervate. The implications of this evidence for current theories of elastin structure are discussed.

† Supported by USPHS under grant number NIHD 00669.

†† We are grateful to Prof. L. B. Sandberg, University of Utah Salt Lake City, Utah 84112 for our sample of tropoelastin.

1. H. G. Bungenberg de Jong in H. R. Kruyt "Colloid Science", Vol. 2, Ch. VIII (Elsevier, Amsterdam, 1949).

W-PM-G2 COACERVATION OF REPEAT SEQUENCES OF ELASTIN. M. M. Long*, D. W. Urry, B. A. Cox*, T. Ohnishi*, and M. Jacobs*, Laboratory of Molecular Biophysics and the Cardiovascular Research and Training Center, University of Alabama in Birmingham, Birmingham, Alabama 35294.

There are in α-elastin, repeat sequences of a tetramer, pentamer, and hexamer, Val-Pro-Gly-Gly, Val-Pro-Gly-Val-Gly, and Ala-Pro-Gly-Val-Gly-Val (Foster, J. A., Bruenger, E., Gray, W. R. and Sandberg, L. B., J.B.C. 248, 2876, 1973; Gray, W. R., Sandberg, L. B. and Foster, J. A., Nature, 246, 461, 1973). This laboratory synthesized polymers of these peptides and found them to be models appropriate to the study of the physical properties of elastin. As does elastin, these three polymers, i.e. the 4n, 5n, and 6n peptides, coacervate. For example, the polypentapeptide will coacervate in the same temperature range as α-elastin (27°C to 37°C). Also, high resolution EM has shown the coacervate of the 5n polymer to be filamentous, as are the coacervate of α-elastin and tropoelastin. Circular dichroism (CD) spectra of the synthetic high polymer in TFE and in its coacervated state are similar, while the spectrum in water is qualitatively and quantitatively different and relatively temperature insensitive at 1 mg/ml peptide concentration. These data indicate that the coacervate of the repeat pentapeptide results primarily from intermolecular as opposed to intramolecular hydrophobic interactions. (Supported by NIH Grant HL-11310).

W-PM-G3 IMMUNOLOGIC DETERMINANTS IN ELASTIN OF MATURE BOVINE LIGAMENT. K. Nishiie*, M. Paz* and S. Seifter, Department of Biochemistry, Albert Einstein College of Medicine, Yeshiva University, Bronx, New York 10461.

Elastin prepared from ligamentum nuchae by an autoclaving procedure was subdivided into component parts or degraded, or both. Resulting defined materials used for immunization and/or subsequent reactions with raised antisera were: Whole ground elastin (I); elastin solubilized in hot oxalic acid (II); coacervated fraction of oxalated elastin (III); non-coacervated fraction (IV); "microfibrillar"elements prepared by solubilization with dithiothreitol (V) or $NaHSO_3$ (VI); "amorphous", insoluble fractions remaining after removal of material with dithiothreitol (VII) or $NaHSO_3$ (VIII); limit peptides, containing desmosine and isodesmosine crosslinks, obtained by digestion with pronase (IX); and limit crosslinked peptides coupled with methylated bovine serum albumin (X). In rabbits, poor antibody response was obtained in 8 weeks when antigen was mixed with Norit, but good response with complete Freund's adjuvant. Antisera were tested variously by double immunodiffusion, immunoelectrophoresis, complement fixation, passive hemagglutination, inhibition of complement fixation and hemagglutination, and radioimmunoassay. When results were positive, correlations among different tests were good. Contrary to expectation, immunogenicity was associated with the "amorphous" part of this kind of elastin. There was cross-reactivity among I, II, III, IV, VII and VIII in appropriate combinations with antisera. Limit peptides, alone (IX) or conjugated (X), did not elicit specific antibodies, did not react with antisera to various fractions of elastin, nor inhibit appropriate antigen-antibody reactions. In summary, the expressed antigenic determinants were located in the "amorphous" part of the mature fiber apart from the peptide segments with the crosslinking desmosines. Antibodies were both of the IgG and macromolecular types. (Aided by NIH grant AM 11913.)

W-PM-G4 THE ROLE OF IONIC INTERACTION IN DESTABILIZING THE TRIPLE HELIX OF A COLLAGEN MODEL SYNTHETIC POLYHEXAPEPTIDE. G. F. Sigler and A. G. Walton, Department of Macromolecular Science, Case Western Reserve University, Cleveland, Ohio 44106.

Poly(Lys(HBr)GlyProProGlyPro) has been synthesized and studied by circular dichroism spectroscopy. It is apparently the first polyhexapeptide collagen model reported with an ionizable side chain. The monomer (ε-(p-NO_2Z)LysGlyProProGly-Pro-ONP) [i.e., p(NO_2)Z = p-nitrobenzyloxycarbonyl -ONP = p-nitrophenylester] was prepared by a stepwise strategy employing active esters. Polymerization in DMF followed by removal of the Lys side chain protection with HBr/acetic acid gave a polydisperse product. Fractionation was accomplished by gel filtration chromatography. The polydisperse material has a molecular weight (M_n = 5-17,000) and (M_w = 5-19,000). High molecular weight fractions form triple helices under concentrated conditions at 5°C. The triple helical structure gives a CD pattern very similar to that of collagen and its triple helical analogs. A high molecular weight fraction ($3xM_n$ = 48,000) was found to melt at 42°C at neutral pH but increased to 54°C at pH 12 where the lysyl side chains are predominantly deprotonated. Furthermore, reconstitution of triple helices appeared to be more readily achieved at high pH. Thus, it is concluded that ionic repulsion between side chains causes destabilization of the triple helix and hinders reconstitution.

W-PM-G5 FLUORESCENCE STUDIES OF THE INTERACTION OF HYALURONIC ACID AND ACRIDINE ORANGE. B. Chakrabarti, Dept. of Connective Tissue Research, Boston Biomedical Research Institute, Boston, Massachusetts 02114.

The interaction of hyaluronic acid with acridine orange has been investigated by fluorescence studies. Upon binding to hyaluronic acid, the intensity of fluorescence of acridine derivation at all wavelengths of excitation and emission decrease when the polymer-dye ratio (P/D) increases. There is a variation in the nature of quenching curves (F/Fo-1 Vs P/D) when the concentration of dye is altered (from 10^{-7} to 10^{-5} M). From the nature of binding curves, absorption and fluorescence spectra of the complex and quantum yield, it appears that the interaction of dye with polymer is primarily electrostatic. The exciton-like CD band of hyaluronic acid-acridine orange complex has been attributed to helical structure of hyaluronic acid. (Chakrabarti and Balazs, BBRC 52:1170, 1973) The observed difference in quenching curves at various concentrations of dye in polymer-dye complex suggests that the dye-dye interaction in presence of hyaluronic acid can either be non-resonance or exciton-type depending upon the conformation of the polymer and the available anionic sites. Supported by NSF Grant No. GB-40666 and PHS Grant No. EY00223.

W-PM-G6 X-RAY DIFFRACTION STUDIES OF THE STRUCTURE OF CELLULOSE MICROFIBRILS. F.J. Kolpak* and J. Blackwell, Department of Macromolecular Science, Case Western Reserve University, Cleveland, Ohio 44106

Electron microscopy has shown that all native cellulose microfibrils are arrays of elementary fibrils, 35Å in width. The major difference between celluloses from various sources lies in the degree of perfection of this array, which will determine many of the physical and mechanical properties. We have calculated x-ray diffraction patterns of cellulose microfibrils, built up by convoluting the elementary fibril with perfect and distorted lattices. The results show that significant distortions can be incorporated into the packing of the elementary fibrils without producing unacceptable changes in the small angle and wide angle x-ray intensity distributions. This work gives an indication of the type of disorder possible in cellulose microfibrils.

W-PM-G7 CONFORMATIONAL ANALYSIS OF SIX MUCOPOLYSACCHARIDES. R. Potenzone Jr. and A.J. Hopfinger, Department of Macromolecular Sciences, Case Western Reserve University, Cleveland, Ohio 44106.

Empirical potential energy functions (EPF) were used to examine a general conformational model for the 1,4'linkage of mucopolysaccharides. (MPS). Agreement with accepted xray structures of cellulose and xylan was found. Further characterization of the 1,4' linkage was conducted using the CNDO/2 technique on a model compound. The bond angle was studied and general agreement with the Arnott and Scott experimental results was found. The torsional energy contributions of orbital deformations was calculated yielding an extremely complex surface. In a similar manner, the less studied 1,3' linkage was examined. Using CNDO/2, the residual electronic charges were calculated, piecewise, on the six MPS, hyuluronic acid, chondroitin, chondroitin-6-sulfate, chondroitin-4-sulfate, dermatan sulfate and keratan sulfate. The monomer of each of these, defined as the 1,4' linked dissacharide was then extensively studied for all rotation al degrees of freedom, using the EPF. The results indicated a rotationally restricted monomer unit. These monomers were then linked through a 1,3' linkage to form the polymer. A trisaccharide was used to consider the chain conformational properties of these polymers, for rotation about the 4 main chain bonds. The side groups were rotated to a minimum energy position. The associated helical parameters for the resulting allowed and preferred conformational states were calculated and compared to current x-ray data. These results were also compared to certain available experimental hydrodynamic properties as well as recent IR and Raman data.

W-PM-G8 QUANTITATIVE ELECTRON MICROSCOPY OF MICROTUBULE ASSEMBLY *IN VITRO* M. W. Kirschner*†, L. Honig*‡ and R. C. Williams‡, †Dept. of Biochemical Sciences, Princeton Univ., Princeton, NJ 08540, and ‡Dept. of Molecular Biology and Virus Laboratory, Univ. of California, Berkeley, CA 94720.

Microtubule assembly was studied by quantitative electron microscopy. Specimen material was deposited upon glowed carbon films by spraying from a nebulizer which mixed the protein solution and stain (6% UrAc) during spraying. Droplets of $\sim 10^{11}$ ml were produced, which spread into patterns small enough to be wholly photographed at $\sim$×8000 in one exposure. Droplet volumes were quantified by adding bushy stunt virus at known concentration to the protein solution. In each droplet pattern the recognizable double rings and spirals were counted, and the lengths of assembled microtubules and helical ribbons (5 to 10 protofilaments) were measured. From the known masses, or mass/unit length, of these species the percentage of protein assembled in these forms was determined. Starting material was cold-depolymerized microtubule protein from porcine brain, at 0.8 mg/ml, in 0.05M ammonium acetate, pH 6.4, containing .5mM $MgCl_2$ and 1mM EGTA, and warmed to 37°. Assembly was initiated by addition of GTP to 1mM. The Table shows average results of two experiments. It is seen that rings and spirals have almost disappeared within about 3 min. Helical ribbons increase for about 4 min and then disappear. They are evidently an intermediate in assembly. The results support a model wherein rings and spirals are converted into protofilaments which progressively aggregate laterally and finally form cylindrical microtubules.

Time (min) after GTP addition	Relative mass (%)		
	Rings and spirals	Helical ribbons	Microtubules
0	24	0	0
1	10	5.4	3.0
3.5	0.1	13	17
9	0	1.9	38

W-PM-G9 MICROTUBULE PROTEIN SYNTHESIS DURING CILIUM DEVELOPMENT. Ilona Staprans and Ellen Roter Dirksen*. Cancer Research Institute, University of California, San Francisco, California 94143.

In the developing mouse oviduct tubulin pools are present during the period when ciliary axonemes are being formed (3-12 days after birth). Experiments were performed to determine if the tubulin assembled into the oviduct cilia is derived from the preexisting pool or is synthesized during development. Tubulin synthesis was determined by measuring the incorporation of ^{3}H-lecuine into tubulins of the soluble, particulate and axonemal fractions of mouse oviduct homogenates. Each oviduct fraction was electrophoresed on SDS gels and the specific activity of the tubulin band determined. Pulse labeling experiments, where ^{3}H-leucine was injected into newborn mice or where it was added to the isolated oviducts in culture, showed that tubulin synthesis occurred throughout development. Incorporation was highest in the youngest animals (3 days) in all fractions. At 5 days, synthesis dropped to about 50% of the earlier high value and remained at this level throughout development, thus maintaining a constant tubulin pool. Isotope dilution experiments demonstrated that at least 70% of this pool is synthesized de novo while cilia are being formed. When ^{3}H-leucine was injected, the highest amino acid incorporation occurred into the axonemal fraction even as early as 3 days. However, in culture, the axonemal fraction showed very little incorporation, suggesting that additional, possibly hormonal control is required for normal morphogenetic events to occur. Amino acid incorporation was sensitive to cyclohexamide, but no significant effect could be obtained with colchicine concentrations below 10^{-3}M. We conclude that constant de novo synthesis of tubulin is required in order to maintain large tubulin pools during cilium formation in the developing mouse oviduct. (Supported by USPHS Grant HD-06374).

W-PM-G10 THE BINDING OF VINCA ALKALOIDS TO CALF BRAIN TUBULIN. James C. Lee, Debra Harrison* and Serge N. Timasheff, Grad. Dept. of Biochemistry, Brandeis Univ., Waltham, Mass. 02154.

The interactions between calf brain tubulin and the anticancer drugs, vinblastine sulfate and vincristine sulfate, were studied by ultracentrifugation, fluorescence and gel filtration in 0.01 M phosphate buffer, pH 7.0, in the presence of 10^{-4} M GTP. The velocity sedimentation patterns were analyzed in terms of the theory of Cann and Goad (J.R. Cann and W.B. Goad, Arch. Biochem. Biophys. 153, 603-609, 1972). The results indicate that 2×10^{-5} M vinblastine sulfate induces dimerization of the stable calf brain tubulin dimer (M.W. 110,000). The binding constants and stoichiometry of the tubulin-drug interactions were examined by the quenching and enhancement of intrinsic and extrinsic fluorophores, respectively, and the tubulin-vinblastine interaction was also investigated by a modified Hummel-Dreyer gel filtration technique. The two types of measurements gave close to identical values of the association constant, $K=2.5\times10^{4}$ M^{-1} at 25° and a stoichiometry of two binding sites for vinblastine sulfate per tubulin dimer of M.W. 110,000. (This work was supported by NIH grant GM-14603, NSF grant GB-38544X and a grant from the Amer. Cancer Soc., Mass. Division).

W-PM-G11 THE MAGNESIUM-INDUCED SELF-ASSOCIATION OF CALF BRAIN TUBULIN. Ronald P. Frigon* and Serge N. Timasheff, Grad. Dept. of Biochemistry, Brandeis Univ., Waltham, Mass. 02154.

The self-association of calf brain tubulin has been studied as a function of magnesium ion concentration by velocity ultracentrifugation. At pH 7.0 and 20°, at protein concentrations below 10 mg/ml, a single peak is observed at Mg^{++} concentrations below 8×10^{-3} M; the sedimentation coefficient of the peak, however, gradually increases with both magnesium ion and protein concentration. At higher Mg^{++} concentrations, the sedimentation pattern becomes bimodal at already low protein concentrations, the area distribution under the two peaks varying as a regular function of protein concentration. Analysis of these results in terms of the Gilbert theory has shown that tubulin, in the presence of magnesium ions, undergoes a progressive self-association of the 5.8 S 110,000 mol. wt. dimers. The end-product is a closed polymer with a sedimentation coefficient of 42 S, composed of 26 ± 4 tubulin dimers. Analysis of the hydrodynamics in terms of the Kirkwood theory indicates a closed ring geometry of dimensions similar to those of ring-like structures seen in the electron microscope. This self-association is characterized by a positive enthalpy, positive entropy, positive heat capacity, positive molar volume change and a first power dependence on magnesium ion activity. (This work was supported by NIH grants GM-14603, GM-212, NSF grant GB 38544X and a grant from the Amer. Cancer Soc., Mass. Division).

W-PM-G12 THE SYNTHESIS OF TUBULIN IN A HETEROLOGOUS CELL-FREE SYSTEM USING ISOLATED TUBULIN mRNA. M. A. Gilmore* and S. M. Heywood, Genetics and Cell Biology Section, University of Connecticut, Storrs, Connecticut, 06268.

Tubulin has been synthesized in a heterologous cell-free system consisting of a rabbit reticulocyte lysate, messenger RNA obtained from 14 day embryonic chick brain and specific initiation factors from either embryonic chick brain or muscle. The tubulin mRNA is obtained from the 18-20S RNA fraction isolated from polysomes consisting of from 10-30 ribosomes per polysome. The tubulin mRNA is further purified by oligo(dT) cellulose chromatography. Messenger RNA, derived in this manner, directs the incorporation of ^{35}S-methionine into a protein which a) participates in two cycles of polymerization and depolymerization characteristic of tubulin; b) is precipitable with vinblastine, and c) co-migrates with *in vitro* synthesized tubulin upon SDS-acrylamide gel electrophoresis. In addition, electrophoretic analysis suggests that both subunits of tubulin are synthesized. In order to investigate the role of specific initiation factor fractions on tubulin synthesis in this system, the phosphocellulose fraction of IF3 (eluting at 0.35M phosphate)-previously shown to stimulate myosin synthesis - was added to the cell-free system. This fraction of IF3 from either brain or muscle is found to stimulate tubulin synthesis 3-4 fold. (Supported by NIH Grant # HD 03316).

W-PM-G13 PRESSURE-INDUCED DEPOLYMERIZATION OF BRAIN MICROTUBULES IN VITRO. Edward D. Salmon*, (Intr. by Edward F. MacNichol), Marine Biological Laboratories, Woods Hole, Massachusetts 02543.

In a variety of cell types, moderate hydrostatic pressure (3,000 psi to 10,000 psi) rapidly depolymerizes "labile" microtubules such as those of the mitotic spindle. For comparison to in vivo studies, the pressure dependence of microtubule assembly was studied in vitro using rabbit brain tubulin purified by two cycles of assembly-disassembly in a buffer containing 0.1 M MES, 1 mM EGTA, 0.1 mM DTT, 0.5 mM $MgCl_2$, and 2 mM ATP. Polymerization was assessed with polarization and electron microscopy and monitored directly using turbidity as a measure of the mass of assembled tubulin. At 22°C, 8,000 psi causes complete depolymerization within 2 minutes. Increasing the temperature increases the pressure required: 10,000 psi is necessary at 29°C, hence the effects of pressure and low temperature are synergistic. The pressure induced depolymerization is reversible. Although at 22°C repolymerization is extremely slow, at 29°C the microtubule assembly returns to approximately its original equilibrium level within 14 minutes and many depolymerization-polymerization cycles can be made. For pressures less than that required to produce complete disassembly, the microtubules depolymerize to equilibrium levels dependent on the magnitude of pressure and temperature. The rate of microtubule disassembly increases progressively with higher pressure, the kinetics appearing to be first order. The apparent activation volume is about -75 ml/mole at 29°C. The results of these experiments are compatible with observations and analyses of the effects of pressure on in vivo microtubules and indicate that pressure affects the association of tubulin subunits directly without requiring some intermediate mechanism. (Supported in part by grant GM20644-01 from NIH).